Adaptive Tuned Vibration Absorber

by

Rodney D. Red Wing

Thesis submitted to the Faculty of the

Virginia Polytechnic Institute & State University

in partial fulfillment of the requirements

for the degree of

Master of Science

in

Mechanical Engineering

APPROVED:

Dr. H.H. Cudney, Chairman

Dr. R. Mitchiner

Dr. H. H. Robertshaw

January, 1997

Blacksburg, Virginia

Keywords: vibrations, control, structures, dynamics, adaptive control

Adaptive Tuned Vibration Absorber

by

Rodney D. Red Wing

Committee Chair: Harley H. Cudney

Mechanical Engineering Department

Abstract

A control algorithm is developed and applied to a previously designed tunable vibration absorber. The adaptive vibration absorber is capable of detecting the frequency of the driving force and tuning itself automatically to that particular frequency. The primary structure was previously designed to obtain a certain natural frequency. The absorber structure was previously designed so that its range of frequencies includes the natural frequency of the primary structure. The primary structure design consists of a cantilever beam with the absorber attachment hardware, and the vibration absorber assembly consists of three rods and a stepper motor.

The control algorithm uses a look-up table and a gradient search to optimize the effectiveness of the absorber for vibration reduction on the primary structure. The look-up table uses an equation, based on experimental data, to transform a given voltage input, directly proportional to the forcing frequency, into an output command necessary to adjust the natural frequency of the absorber. Once the input voltage reaches a steady state, the gradient search routine adjusts the natural frequency of the absorber to ensure the absorber is tuned to the optimal frequency that minimizes the primary structure vibration.

The primary structure with the adaptive absorber offers significant reduction to the vibration amplitudes of the primary structure, as compared to both the primary structure with no absorber and the primary structure with a passive absorber, throughout the 45 Hz

to 71 Hz and 73 Hz to 108 Hz range. The primary structure with no absorber has a 1st mode natural frequency of 72 Hz and offers the lowest vibration amplitudes, as compared to both the primary structure with the adaptive absorber and the primary structure with a passive absorber, throughout the ranges of 30 Hz to 45 Hz and 108 Hz to 130 Hz. The primary structure with the passive absorber offers the lowest vibration amplitudes of the primary structure, as compared to both the primary structure with no absorber and the primary structure with the adaptive absorber, throughout the 71 Hz to 73 Hz range.

Acknowledgments

Although much work is performed by the master's candidate, I would not have accomplished this thesis without the efforts and motivation of many people. I would most like to thank Prof. Harley H. Cudney for being my advisor and committee chair. With his guidance and understanding, I accomplished more than I ever dreamed possible. I would also like to thank Prof. Harry H. Robertshaw and Prof. Reginald G. Mitchiner for being on my committee and offering their support when needed. I also thank Prof. Al Wicks for his help with data analysis and for providing needed instrumentation.

I give special thanks to the GEM Consortium for providing me with a fellowship. In addition, I thank both the Graduate School and the Mechanical Engineering Department at Virginia Tech for complementing the GEM fellowship. I would also like to thank General Motors, especially the Noise and Vibration Center at the General Motors Proving Ground for being the corporate sponsor of the GEM fellowship and providing a wonderful and fulfilling place to work during my internships.

I would like to thank my co-workers and friends in the laboratory; Anton Sumali, Chris Niezrecki, Dave Schmiel, and Larry Tentor. I especially want to thank my partner, Ana Moyka, who was there throughout most of the madness.

I thank my brother and sister in-law, Ronald and Joan Redwing, for their influence and periodic financial support. I also thank my parents, grandmother, and my uncle Wesley Hilburn for assisting me when I needed it most.

Last but not least, I thank my family; Robin Red Wing, and Kaitlyn Red Wing for believing in me and standing by me throughout my graduate education.

Table of Contents

List of Figures

List of Tables

Nomenclature

c_1	primary structure damping constant
c_2	absorber structure damping constant
F_o	magnitude of disturbing force
F_t	force transmitted to base
k_1	primary structure spring stiffness
k_2	absorber structure spring stiffness
m_1	primary structure mass
m_2	absorber structure mass
μ	mass ratio, m_2/m_1
ς_1	primary structure damping ratio
ς_2	absorber damping ratio
P	absorber motor position
R	frequency ratio, ω_2/ω_1
S	absorber motor step value
t	time
V	input voltage value
ω	forcing frequency
ω_r	resonant frequency
ω_1	natural frequency of primary structure
ω_2	natural frequency of absorber structure
ω_{11}	first natural frequency of combined system
ω_{22}	second natural frequency of combined system
X_1	primary structure coordinate
X_2	absorber structure coordinate

Chapter 1

1. Introduction

In this chapter we will review the motivation for this project. Next, we will review other work with adaptive vibration absorbers that use some method of control. We will also include a statement of how our work complements the work of others. The objective and approach to the adaptive absorber are also presented. Finally, the outline of the thesis is presented.

1.1 Motivation

Vibration suppression in structures with varying forcing frequencies is of interest in areas such as the automotive and aerospace industries. Vibrations often excite panels and other components to create obtrusive and potentially dangerous noise levels. In other instances, the vibration levels cause fatigue failure, wear, and component damage. In this project we want to suppress the vibration levels of a primary structure throughout a frequency range. Lower vibration levels in turn improve the perceived quality, safety, and useful life of various structures. The use of a tuned vibration absorber (TVA) is a potential way to suppress vibrations.

Some current structures have passive TVA's that are tuned to either the natural frequency of the structure or a non-varying forcing frequency. Passive TVA's that are tuned to the natural frequency of a structure become untuned when the structure or absorber characteristics change. Typically the primary structure is a more complex design than the absorber structure, allowing for the primary structure characteristics to be at a greater risk of changing over time. However, the absorber characteristics changing over time is also a concern. These changes can be due to material changes from weathering and/or fastened

locations becoming less rigid. We will address the situation where there is a varying forcing frequency, therefore the passive TVA that is tuned to a non-varying forcing frequency is not appropriate.

There is a need to develop absorbers that remain tuned to a varying forcing frequency throughout a frequency range that includes a natural frequency of the primary structure. Even if the primary structure's natural frequency was to change slightly, the absorber range should still include the primary structure's natural frequency. If the absorber natural frequency was to change then a closed loop algorithm could be implemented to optimally tune the absorber to the forcing frequency when the forcing frequency reaches a non-varying state.

1.2 Literature Review

A distinction between passive, adaptive, and active vibration absorbers must be made in order to provide the reader with reasons why we consider our vibration absorber to be an adaptive vibration absorber.

First, a **passive** vibration absorber is tuned near or at frequencies associated with the modes that we want to eliminate and the absorber can also add damping to the structure (Sun *et al.*, 1995). Passive absorbers are acted on by the primary structure as opposed to the absorber acting on the primary structure. Passive TVA's are effective only when the tuning and damping are appropriate for particular operating and environmental conditions. Because these conditions often change with time, passive TVA's may become mistuned and lose their effectiveness (Sun *et al.*, 1995).

Second, **adaptive** absorbers have controllable or adjustable parameters such that their behavior can be tuned automatically over time (Sun *et al.*, 1995). An adaptive TVA detects the forcing frequency and changes its parameters to suit the condition.

Lastly, **active** absorbers consist of an active element parallel to a resilient element that supports a reaction mass. The active element produces a force acting on the reaction mass (Sun *et al.*, 1995). The active TVA produces a force acting on the primary structure rather than allowing the primary structure to act on the absorber. Energy is required to supply this force; thus, active TVA's supply energy at the same time they dissipate energy (Walsh *et al.*, 1992). In addition, they are often part of an active control algorithm (Sun *et al.*, 1995).

The previous work applicable to this research is in the area of adaptive tuning of a vibration absorber. In this section, we present to the reader background information involving absorbers that are tuned adaptively. Our objective is to present knowledge of what has been accomplished to date regarding the types of control techniques used and by whom in adaptive TVA's and how this thesis complements and adds to the research already accomplished.

Sun *et al.* (1995) present an overview of passive, adaptive, and active TVA's. The paper offers a brief description on the recent progress of adaptive TVA's, along with their on-line tuning strategies. The paper begins by discussing fundamental aspects of TVA's. They continue by discussing some contemporary applications of TVA's and conclude by discussing recent works on adaptive TVA's as well as active TVA's. The most important part of this paper is the section on adaptive TVA's and the control strategies used for these TVA's. Sun *et al.* (1995) present three different control approaches that have been extensively studied.

Ryan *et al.* (1994) use a classical feedback control scheme applied to an adaptive vibration absorber (Fig. 1.2-1). The authors state that current self-tuning absorbers use feedforward approaches that are open loop control. Since airspeed, temperature, and altitude can influence the behavior of their vibration absorber, they propose that an open loop scheme

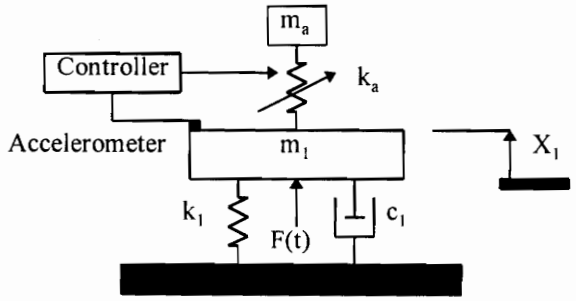

Figure 1.2-1: Representation of Ryan *et al.* Adaptive Vibration Absorber

would result in poor performance. The feedback tuning scheme presented is insensitive to variations in the excitation frequency and system parameters. This robust performance is realized by adding a self-tuning capability to vibration absorbers. In this paper, the experimental verification of this proposed tuning scheme is presented. To achieve the maximum attenuation of steady state vibration amplitudes, the absorber has almost no damping and continuous self-tuning capabilities. The input to the primary structure is the harmonic disturbance force. The output is the acceleration of the primary structure as read by an accelerometer. The accelerometer is used as the feedback sensor to create a DC signal indicating the degree of mistuning. A proportional controller is used to change the stiffness of the absorber. The authors present an analog electrical circuit to implement the feedback controller (Fig. 1.2-2). The input to the circuit is the accelerometer signal, Vacc, which is filtered and sent through a rectifier and capacitor to create a DC signal that represents the vibration amplitude. The proportional gain controller uses the DC signal to select a gain value based on the desired tuning rate of the absorber. A higher gain corresponds to a faster tuning rate. A control signal, u, is

applied to the power transistor to drive the absorber motor. The absorber motor acts as an actuator to adapt the stiffness of the absorber by connecting a helical coil to a gear train and changing the number of active coils used by the absorber. From their experiments, the adaptive absorber achieved 25 dB of attenuation. The feedback control tuning enhanced the performance of the passive absorber.

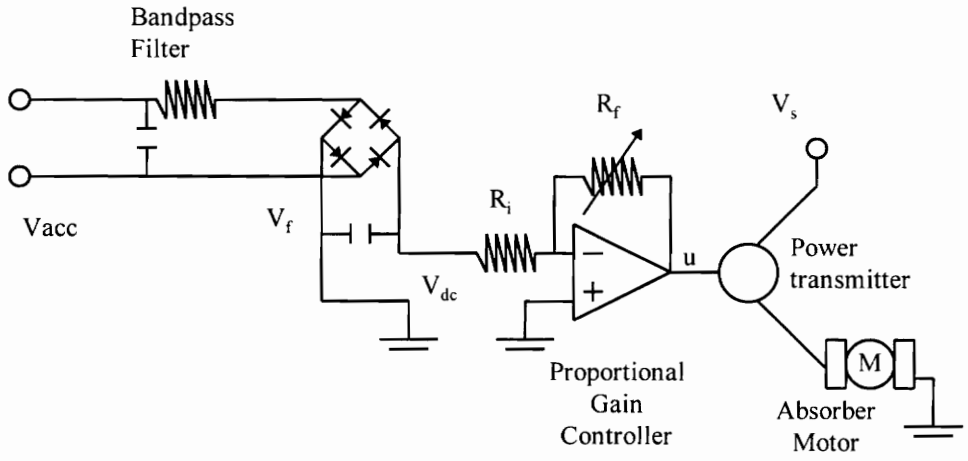

Figure 1.2-2: Analog Circuit Diagram of Ryan *et al.* Feedback Controller

Franchek *et al.* (1993) present a numerical study integrating feedback control with a prototype adaptable vibration absorber. Preliminary results for adaptive passive noise and vibration control techniques are reported. This paper served as the numerical study for the Ryan *et al.* (1994) paper. The same control technique was used as the Ryan *et al.* (1994) paper.

Walsh *et al.* (1992) use a design of an adaptable vibration absorber with a known or learned excitation acceleration and deceleration to minimize transient vibrations during start-up and shut-down of a rotating machine. Also, the absorber adapts to changes in steady state operating speeds that occur when the machine's load condition varies. The objective is to find a variation in stiffness of the absorber as a function of time which will best reduce the vibration amplitude of the main mass during the acceleration, deceleration

and constant speed of the excitation frequency. The authors perform an analytical study of their adaptable vibration absorber. They do not use any feedback controls. Their vibration absorber design is a compound leaf spring. Two strips of sheet metal make up the spring. The two strips are clamped at each end with identical lump masses. The effective stiffness between each end and the center of the strip are varied by separating the leaf springs at the middle. The authors propose that this process can be accomplished by using a stepper motor and a simple lead screw mechanism. The absorber gave a 66 percent improvement in the rms displacement and a 67 percent improvement in peak displacement of the main mass.

DiDomenico (1994) uses a reduced order neural network control strategy for tuning an adaptive absorber (Fig. 1.2-3). The author investigates four optimal tuning strategies.

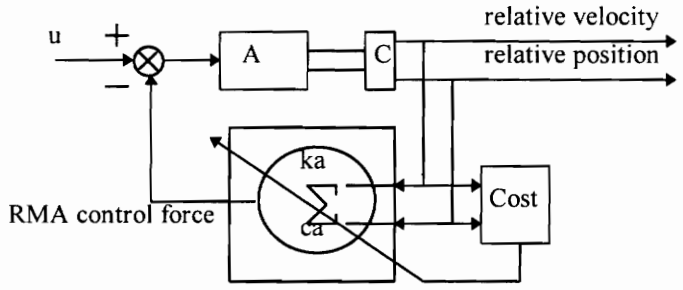

Figure 1.2-3: Flow Diagram of DiDomenico's Single Neuron RMA Controller

The Quasi-Newton (BFGS), Simplex, Least Mean Square (LMS), and backpropagation are the methods investigated. The unsupervised LMS and backpropagation methods were unstable. The neural network control using quasi-Newton or simplex methods gave superior performance as compared to a Den Hartog method presented. The Den Hartog method is a linear method that chooses spring stiffness and damping coefficients to match vibration modes. The author suggests that the reduced order neural network control strategy demonstrates better settling time and energy dissipation than linear design methods. For the neural network control strategy used the spring stiffness and passive

damping of a reaction mass actuator (RMA) are "tuned" using total energy as a cost function. The position and velocity are the inputs used to determine the stiffness and damping of the RMA, respectively. The author does not clearly present how the damping and stiffness of the RMA is physically adjusted. A second order NASTRAN structural mode is used to multiply position and velocity by RMA stiffness and damping coefficients, respectively. This creates a feedback force such that the RMA parameters become output feedback gains. When the output gains are multiplied by output parameters and summed they become the control signal. The feedback gains are also the outputs or weights of a single neuron. A single neuron uses two weights to influence the damping and the spring coefficient. The neural network uses neurons that have multiple inputs, a summing function with threshold, and single output. The inputs are weighted by a matrix prior to summation and thresholding. From the experiments, the reduced order neural network controller demonstrated enhanced performance of the adaptive absorber.

Wang *et al.* (1993) perform a simulation of a beam to suppress the quasi-steady state vibrations of flexible structures caused by start-up and shutdown of machines. They use a novel closed-loop algorithm to adapt the stiffness of the simulated absorber. The feedback signals used are the velocity and displacement of the structure as well as the displacement of the absorber mass and speed of the rotating force. The adaptive action is subjected to constraints to suppress the transient vibrations by minimizing energy input into the structure. From simulations, the transient resonance is effectively suppressed with the adaptive absorber as well as the energy level of the beam.

Lai *et al.* (1993) perform a simulation of a beam to suppress the structural vibrations of flexible structures caused by general non-periodic and/or unknown disturbances. They use a novel closed-loop algorithm to adapt the stiffness of a simulated absorber. A controller with multi-objective fuzzy logic is created to reduce the primary structure energy level while constraining the total system energy. The multi-objective requirement

could contradict each other, therefore, the control law is created based on the theory of Fuzzy Systems. The adaptive action is subjected to constraints to suppress the transient vibrations by minimizing energy input into the structure. Recall that a motionless structure has no energy in the structure. From simulations, the transient resonance is effectively suppressed with the adaptive absorber as well as the energy level of the structure.

The applications of tuned vibration absorbers is surveyed by von Flotow *et al.* (1994). In their third section, the authors present the concepts of adaptation for absorbers. In this section, the authors identify three time delays to be concerned with for adaptation of the absorber. These are the logic delay, actuation delay, and the dynamic delay. The logic delay is associated with the time required for signal processing and recognition of the degree of mistuning. These are dominated by the signal processing and the signal to noise ratios. The actuation delay is the time required to change the absorber natural frequency. Changing the absorber natural frequency is accomplished by changing either the mass or the stiffness (or both) of the absorber and this process takes time. The dynamic delay is the delay that occurs once the absorber frequency is changed. Once this change occurs, the vibration state of the absorber must dynamically change to match the disturbance conditions. In other words, the time it takes for the absorber to reach its steady state resonating condition. The last section of the paper presents a survey of adaptation logic and actuation mechanisms. In this section, the authors present how most of the absorbers are adapted. One of the absorbers in operation, absorbers used in the Boeing CH-47C helicopter, uses a tuning logic that compares the phase relationship between the helicopter and the mass of the absorber. It compares the result with a predetermined value for when the absorber is in proper tune. Based on the results, an adjustment to counter weights on a cantilever beam is done with an electric motor. Another absorber, Helmholtz resonator (patent # W092/15088), uses a tuning logic that

compares the phase between the absorber and base. The authors suggests that adjustments are made by changing the absorber mass and the volume of the resonator.

Desanghere *et al.* (1991) use a feedback control technique to optimally adjust an absorber. The authors adjust the absorber based on the maximum rms acceleration of the main system during two swept sine sweeps. The absorber system adjusts its stiffness to reach the optimal tuning point. The stiffness is adjusted by changing the pressure on the PVC rings. The rings are located between their supports on the absorber and the internal wall of the primary structure. The pressure on the PVC rings is adjusted by a pneumatic cylinder connected to an air pressure regulator. The adaptive absorber effectively reduces the maximum acceleration levels observed by the primary structure.

Hollkamp (1994) uses a feedback tuning algorithm that maximizes the ratio of the absorber accelerometer amplitude to the base accelerometer amplitude. The author uses the ratio of rms responses instead of just the rms response of the primary structure so

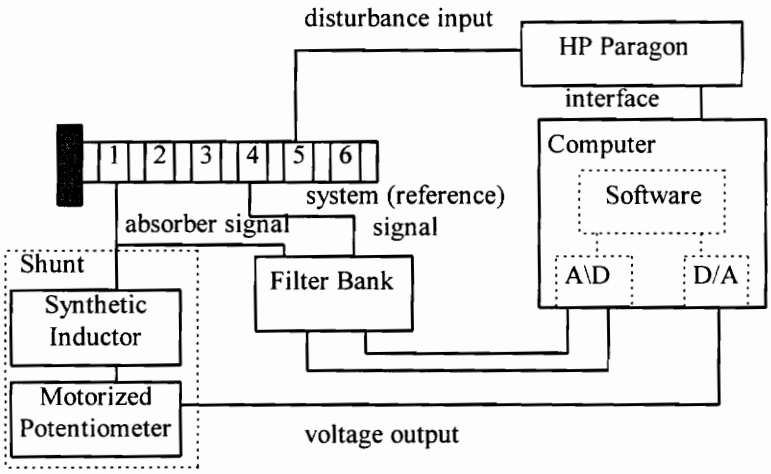

Figure 1.2-4: Schematic of Hollkamp's Experimental Setup

that they do not have to maintain a consistent magnitude for the disturbance force. The absorber is a self-tuning piezoelectric vibration absorber that tracks a particular mode of the beam (Fig. 1.2-4).

For their experiments, they use a cantilevered beam as the primary structure. The tuning is accomplished by adjusting the shunt inductance and resistance. They use a synthetic inductor (Fig. 1.2-5).

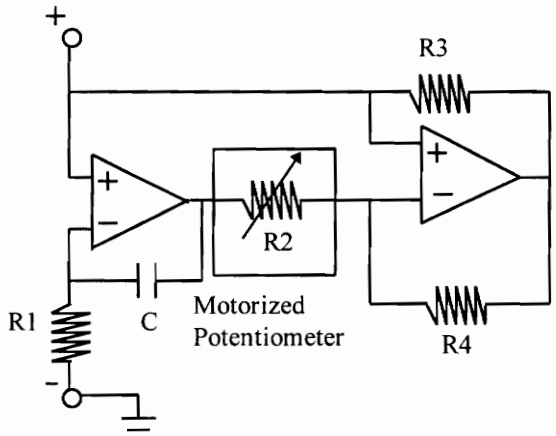

Figure 1.2-5: Synthetic Inductor used by Hollkamp

In summary, we will be using the primary structure acceleration level to optimize our absorber's effectiveness similar to that done by Ryan *et al.* (1994) and Franchek *et al.* (1993). DiDomenico (1994) measures position and velocity to determine the energy level of the primary beam in order to optimize the absorber. Wang *et al.* (1993) also measures position and velocity to determine the absorber adjustment location. Lai *et al.* (1993) measures the structure energy as well as the total system energy level. Hollkamp (1994) measures both the absorber and primary structure acceleration levels to optimize their absorber's effectiveness. Both the absorber used in the Boeing CH-47C helicopter and the Helmholtz resonator, von Flotow *et al.* (1994), compare the phase relationship between the absorber and the primary structure to determine the absorber settings.

We will be using a feedback technique to optimize our absorber structure. Ryan *et al.* (1994), Franchek *et al.* (1993), DiDomenico (1994), Wang *et al.* (1993), Lai *et al.* (1993), Helmholtz resonator (von Flotow *et al.* (1994)), and Hollkamp (1994) use a feedback technique to optimize their system.

In addition to the summary, Ryan *et al.* (1994) along with Franchek *et al.* (1993), DiDomenico (1994), Wang *et al.* (1993), Lai *et al.* (1993) and Hollkamp (1994) present the transient vibration levels of their adapted systems. Ryan *et al.* (1994) present the final dB reduction obtained by the authors adapted system for two particular forcing frequency values; however, they do not state for what frequency range the level of dB reduction would be obtainable. We will be investigating the vibration levels obtained for the primary structure once the absorber has already adjusted to its optimal location throughout a frequency range that will include the resonance of the primary structure. We will also investigate the vibration levels obtained for the primary structure when the forcing frequency is outside the optimal tuning frequency range of the absorber. This differs from the concentration of the previous authors' works. Also, we are not concerned with the speed of adaptation, only the levels of vibration once the adaptation process is complete.

Lastly, Ryan *et al.* (1994) along with Franchek *et al.* (1993), DiDomenico (1994), the absorber used in the Boeing CH-47C helicopter (von Flotow *et al.* (1994)), and Hollkamp (1994) adjust their absorbers by varying the stiffness. Ryan *et al.* (1994) change the stiffness by varying the number of active coils of their absorber spring. Franchek *et al.* (1993) numerically change the stiffness of their theoretical absorber system. DiDomenico (1994) changes the stiffness of a Reaction Mass Actuator. The absorber used in the Boeing CH-47C helicopter, von Flotow *et al.* (1994), adjusts counter weights, using a motor, on a cantilever beam to change the stiffness of their absorber. Hollkamp

(1994) uses piezoelectric tiles to adjust the stiffness of his absorber. We will be varying our absorber stiffness by adjusting the inertial properties of our absorber, which, in turn will change the stiffness of the absorber. There will also be a very slight change in the effective mass of the absorber system. This is similar to the absorber used by the Boeing CH-47C helicopter, von Flotow *et al.* (1994), in that it will behave like a cantilever beam with an adjustment of the location of the mass along the cantilever beam.

There is a need for adaptive absorbers to track a varying forcing frequency and optimally tune the absorber to that frequency. Some primary structures are more concerned with the final acceleration levels obtained by the optimized system rather than the transient vibration level during the optimization process. If it is important to keep costs low, evaluating the acceleration level of only one structure is less costly than having to simultaneously evaluate the acceleration level of two structures.

1.3 Objective and Approach

A plausible solution to this problem would be to adapt an absorber to the forcing frequency throughout a frequency range including the natural frequency of the primary structure. Also, the final acceleration level obtained by the optimized system should be evaluated. In addition, to keep costs low, the acceleration should be evaluated on only one structure. Our objective of this thesis is to create such an absorber. The absorber will adaptively tune to a forcing frequency within a certain frequency range that will include at least one structural resonance of the primary structure to which the absorber is attached. This will allow the absorber to absorb the energy from the primary structure at the tracked forcing frequency throughout a frequency range of the system. Also, an evaluation of the final primary structure acceleration level will be evaluated for a range broader than the absorber tuning range to show the effects of the absorber outside its

tuning range. Finally, the primary structure acceleration will be the only input into the control algorithm to optimize the system.

1.4 Thesis Outline

In Chapter two we will present vibration absorber theory and the control concept. The vibration absorber theory will cover the effects of an absorber on a primary structure, the effects of the mass ratio on a primary structure, the effects of damping in the absorber on a primary structure, and the effects of damping in the primary structure on a primary structure. The control concept will cover the logic behind the table look-up and gradient search routines. In Chapter three we will present the structural design of the primary structure, vibration absorber structure, and the combined system. Chapter three also includes an explanation of the hardware parts of the control system. Chapter four includes a description of the control program, LabView. Also Chapter four includes the table look-up and gradient search portions of LabView. In Chapter five the experimental set-up and procedure are discussed. In Chapter six we will include the results and analysis obtained from our experiments. Finally in Chapter seven, conclusions and recommendations about the research will be presented.

Chapter 2

2. Overview

In Chapter 2 we will cover background information in vibration absorber theory and the control concept used in this project. In the absorber theory section we will present the effect of an absorber on a primary structure, the effect of the mass ratio on the combined system, and the effects of damping in both the absorber and the primary structure on the combined system. In the control concept section we will present the table look-up and the gradient search concept used to describe the system as a closed-loop.

2.1 Vibration Absorber Theory

In order to understand the concept of the absorber, background information on what an absorber is and how the absorber affects the primary structure needs to be understood. In this section we will distinguish between a vibration absorber and a vibration damper as well as the difference between adjusting an absorber and tuning an absorber. Next, we will present how the addition of the absorber to the primary structure changes the one-degree-of-freedom system into a two-degree-of-freedom system. We will also show how the mass ratio of the system affects the combined system resonant frequencies. Finally, we will present the effects of damping in the absorber and the effects of damping in the primary structure on the displacement of the primary structure for the combined system.

Difference between Vibration Absorber & Vibration Damper

Vibration absorbers virtually eliminate vibration amplitudes in primary structures at the absorber's natural frequency. Vibration dampers reduce vibration amplitudes of a primary structure at various frequencies. However, absorbers differ from dampers in that absorbers oppose the exciting force whereas dampers dissipate the vibration energy, usually as heat.

2.1.1 Effect of Absorber on Primary Structure

Figure (2.1) shows a representation of a single-degree-of-freedom (SDOF) structure. A SDOF structure consists of a

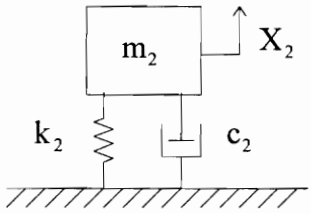

Figure 2.1: Single Degree of Freedom System

spring k_2, mass m_2, and possibly a damper c_2 that when attached to a primary structure becomes an absorber. The absorber is tuned or adjusted to give a primary structure the desired amplitudes of vibration.

Difference Between Adjusting and Tuning an Absorber

Changing the damping of an absorber *adjusts* the amplitudes of vibration of the absorber structure without significantly changing the tuning frequency of the absorber. Using the absorbers differential equation of motion for a forced response, the following absorber vibration amplitude X_2 can be derived

$$|X_2| = \frac{F_o/k_2}{\sqrt{\left[1-(\omega/\omega_2)^2\right]^2 + \left[2\varsigma_2(\omega/\omega_2)\right]^2}}. \qquad 2.1$$

where the absorber damping ratio ς_2 is defined as

$$\varsigma_2 = \frac{c_2}{2\sqrt{k_2 m_2}}. \qquad 2.2$$

When the forcing frequency ω is very near or equal to the absorber natural frequency ω_2, where $\omega/\omega_2 = 1$, equation 2.1 reduces to

$$|X_2| = \frac{F_o/k_2}{2\varsigma_2}. \qquad 2.3$$

In addition, a system with damping has a resonant frequency ω_r defined as

$$\omega_r = \omega_2\sqrt{1-2\varsigma_2^2}. \qquad 2.4$$

It should be apparent from equations 2.3 and 2.4 that for increased values of the absorber damping ratio ς_2 the vibration amplitude of the absorber becomes smaller and the frequency location of the resonant frequency decreases. As compared to a damping ratio of 0.1, a damping ratio of 0.15 has very little effect on the frequency location of the resonant frequency, yet this same change in the damping ratio has quite a significant effect on the vibration amplitude of the absorber. Therefore, changing the damping of an absorber adjusts the amplitudes of vibration of the absorber structure without significantly changing the tuning frequency of the absorber. Whereas, an absorber is *tuned* by varying the absorber's mass m_2 and/or stiffness k_2 as shown by the absorbers natural frequency equation

$$\omega_2 = \sqrt{k_2/m_2}. \qquad 2.5$$

The addition of the absorber to the primary structure creates a combined system having an added degree of freedom as shown in Fig. (2.2). The components of the combined system are: the mass of the primary structure m_1 and the mass of the absorber m_2; the

stiffness of the primary structure k_1 and the stiffness of the absorber k_2; the damping of the primary structure c_1 and the damping of the absorber c_2. There is also an excitation force of $F_o \sin\omega t$ applied to the primary structure mass.

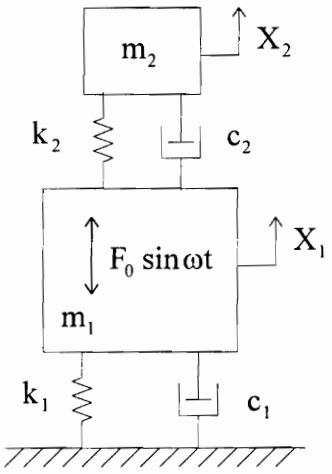

Figure 2.2: Primary Structure With Absorber

When the excitation frequency ω is very near or equal to the natural frequency of the primary structure ω_1 and there is no absorber attached to the primary structure, the amplitude of vibration for the primary structure becomes very large. By tuning the natural frequency of the absorber ω_2 (assuming there is no damping) to that of the excitation frequency ω, the amplitude of vibration of the primary structure X_1 with the absorber reduces to zero (James *et al.*, 1989). This is important since our vibration absorber will have very little damping and we want to eliminate as much of the amplitude of vibration of the primary structure as possible. Damping factors as low as 0.01 are not uncommon in steel and aluminum structural systems (James *et al.*).

The combined system creates two natural frequencies which are dependent upon the mass ratio μ. The mass ratio μ defines the ratio between the absorber mass and the primary structure mass $\mu = m_2/m_1$. The effects of the mass ratio will be discussed later in this

chapter. By assuming harmonic motion, the equation for the primary structure amplitude X_1 can be derived as

$$X_1 = \frac{\left[\frac{F_o}{k_1}\right]\left[1-\left(\frac{\omega}{\omega_2}\right)^2\right]}{\left[1+\frac{k_2}{k_1}-\left(\frac{\omega}{\omega_1}\right)^2\right]\left[1-\left(\frac{\omega}{\omega_2}\right)^2\right]-\frac{k_2}{k_1}}. \qquad 2.6$$

When the forcing frequency is equal to the absorber natural frequency, $\omega = \omega_2$, the primary structure amplitude is zero, $X_1 = 0$. The absorber mass has a displacement amplitude equal to (Thomson *et al.*, 1993)

$$X_2 = -\frac{F_o}{k_2} \qquad 2.7$$

which is 180° out of phase with the harmonic force F_o. The primary structure mass m_1 is subjected to two forces $F_o \sin\omega t$ and $-k_2X_2 \sin\omega t$ which corresponds to a state of static equilibrium at any instant of time. $F_o \sin\omega t$ comes from the excitation force and $-k_2X_2 \sin\omega t$ comes from the force created by the absorber. Therefore, the displacement X_1 of the primary structure is equal to zero for any instant of time (James *et al.*, 1989). In summary, if we can match the forcing frequency with the absorber natural frequency we can eliminate amplitude of vibration of the primary structure.

In our project, the excitation frequency will vary and the absorber will change its natural frequency to match the forcing frequency throughout the absorbers adjustable natural frequency range and change its natural frequency accordingly for forcing frequencies outside the absorbers adjustable natural frequency range. To ensure effectiveness of the

absorber, the range of natural frequencies of the absorber includes the first bending natural frequency of the primary structure.

The following sections will present the effect of the mass ratio on the system; the effect of damping in the absorber on the system; and the effect of damping in the primary structure on the system.

2.1.2 Effect of the Mass Ratio on the System

The mass ratio μ defines the ratio between the absorber mass and the primary structure mass $\mu = m_2/m_1$. When the absorber natural frequency is equal to the primary structure natural frequency, $\omega_1 = \omega_2$, then the mass ratio also equals the ratio of the absorber stiffness to primary structure stiffness $\mu = \frac{k_2}{k_1} = \frac{m_2}{m_1}$. Equation (2.6) for the primary structure amplitude X_1 can then be evaluated as

$$X_1 = \frac{\left[\frac{F_o}{k_1}\right]\left[1-\left(\frac{\omega}{\omega_2}\right)^2\right]}{\left[1-(2+\mu)\left(\frac{\omega}{\omega_2}\right)^2+\left[\left(\frac{\omega}{\omega_2}\right)^2\right]^2\right]}. \qquad 2.8$$

By equating the denominator of the above equation to zero at a known mass ratio, two natural frequencies ω^2 can be found. Figure (2.3) shows the locus of the two natural frequencies of the combined system for different mass ratio values.

For Fig. (2.3), the natural frequency of the vibration absorber is tuned to the natural frequency of the primary structure, $\omega_2 = \omega_1$. This condition corresponds to a natural

frequency ratio equal to unity, $R = 1 = \frac{\omega_1}{\omega_2}$. The two natural frequencies of the combined system are above and below the natural frequency of the primary structure. The first of the two natural frequencies ω_{11} are below the natural frequency of the primary structure. The second of the two natural frequencies ω_{22} are above the natural frequency of the primary structure. From the graph, as the mass ratio becomes larger the two natural frequencies become farther apart (James *et al.*, 1989).

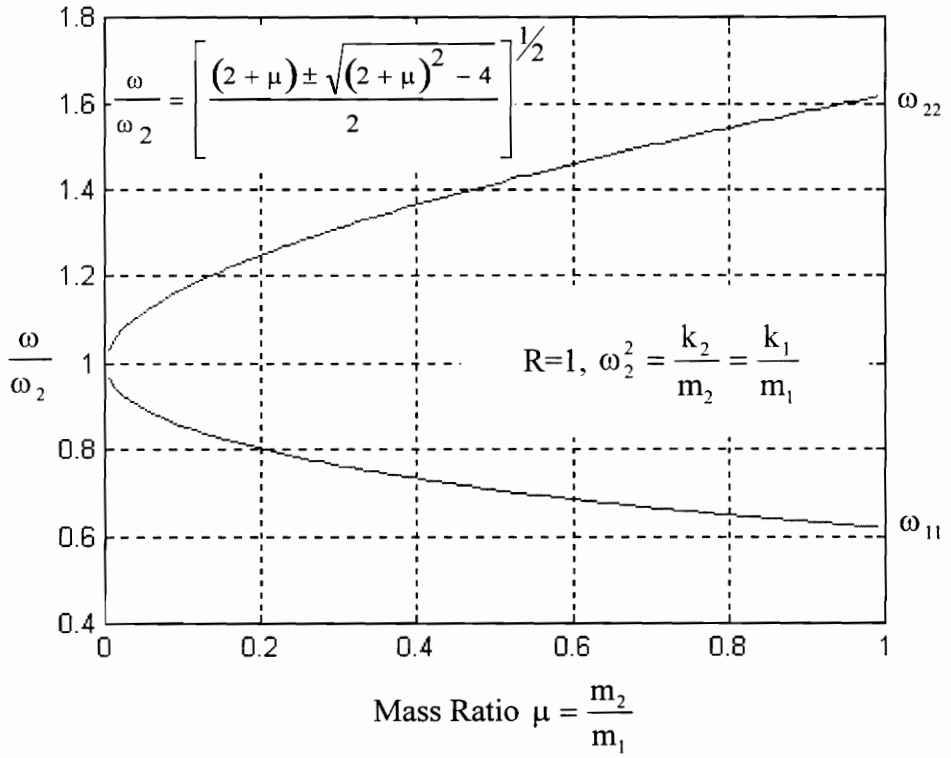

Figure 2.3: Effect of Mass Ratio on Natural Frequencies (James *et al.*, 1989)

It is desirable to keep the two natural frequencies as far apart as possible. If the forcing frequency deviates from the natural frequency of the absorber and the mass ratio is small, the forcing frequency may excite one of the resonant peaks (James *et al.*, 1989).

Figure (2.4) is similar to Fig. (2.3); however, Fig. (2.4) has two additional curves for different primary structure to absorber structure natural frequency ratios. A decrease in absorber natural frequency results in a ratio ω_{11}/ω_{22} greater than one, e.g., R = 1.25. The increased ratio results in a curve that shifts upward and to the left; implying that the two natural frequency resonances are at increased frequencies. An increase in absorber natural frequency results in a ratio ω_1/ω_2 less than one, e.g., R = .833. The decreased ratio results in a curve that shifts downward and to the left, implying that the two natural frequency resonances are at decreased frequencies.

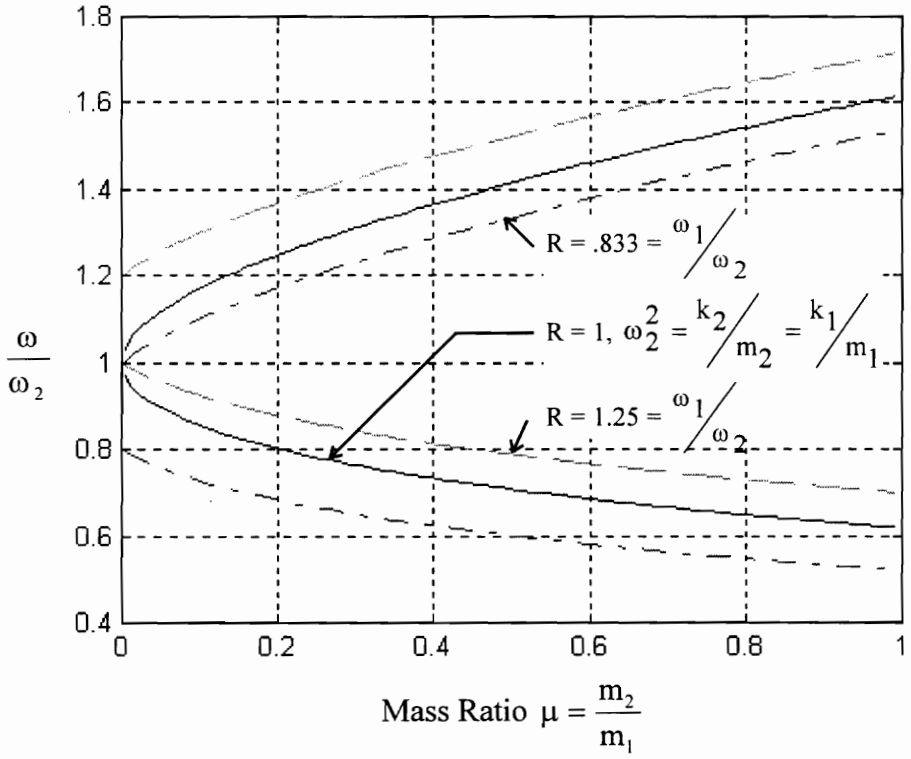

Figure 2.4: Effect of Frequency Ratio on Natural Frequencies

In our project, the resonant frequencies will vary as the absorber changes its natural frequency as well as mass ratio. It is possible to know the locations of the resonant frequencies for various mass ratios and absorber to primary structure natural frequency

ratios; therefore, we are able to determine at which forcing frequencies the absorber should adjust its natural frequency from its highest natural frequency location to its lowest natural frequency location and vice versa. In this project, we will be using experimentally determined resonant frequency values to determine the frequency location to adjust the absorber from its highest frequency location to its lowest frequency location and vice versa.

2.1.3 Effect of Damping in the Absorber

Figure (2.5) shows the effects of varying absorber damping and forcing frequency on the displacement magnitude X_1 of the primary structure in the combined system. The 3-dimensional plot contains primary structure displacement magnitude X_1 as a function of absorber damping ratio ς_2 and forcing frequency ratio. The contour plot shows the same information as the magnitude plot. The absorber and primary structure natural frequencies are equal for the entire plot $\omega_2 = \omega_1$.

By increasing absorber damping, the amplitude of the primary structure for the combined system decreases at the two natural frequency locations. However, the amplitude increases at the original natural frequency of the absorber and primary structure. If the damping continues to increase, the two degree of freedom system begins to behave as a single degree of freedom system with a natural frequency that approaches

$$\omega_1 = \sqrt{\frac{k_1}{m_1 + m_2}}. \qquad 2.9$$

If the absorber has no damping, the combined system has two resonant frequencies. Either resonant frequency could be excited with large magnitudes of displacement if the

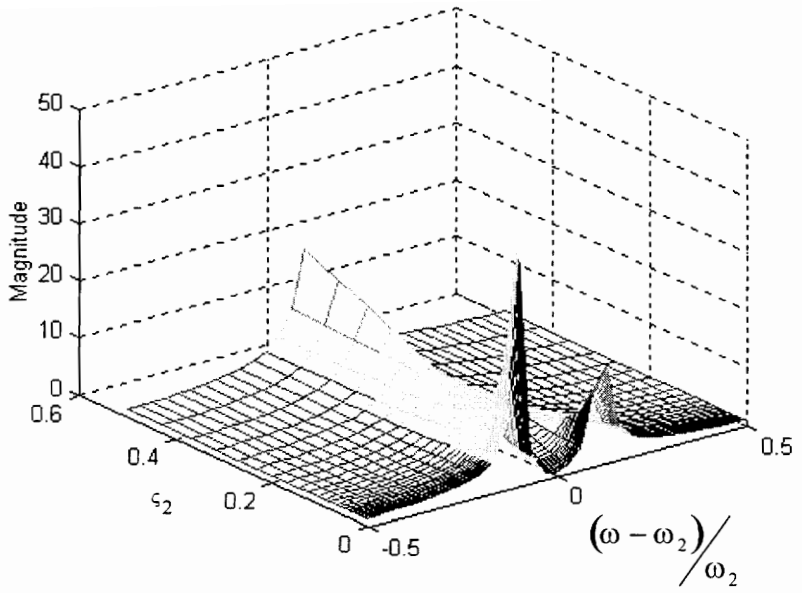

Magnitude, X_1

Figure 2.5 (a): Effect of Varying Absorber Damping and Forcing Frequency

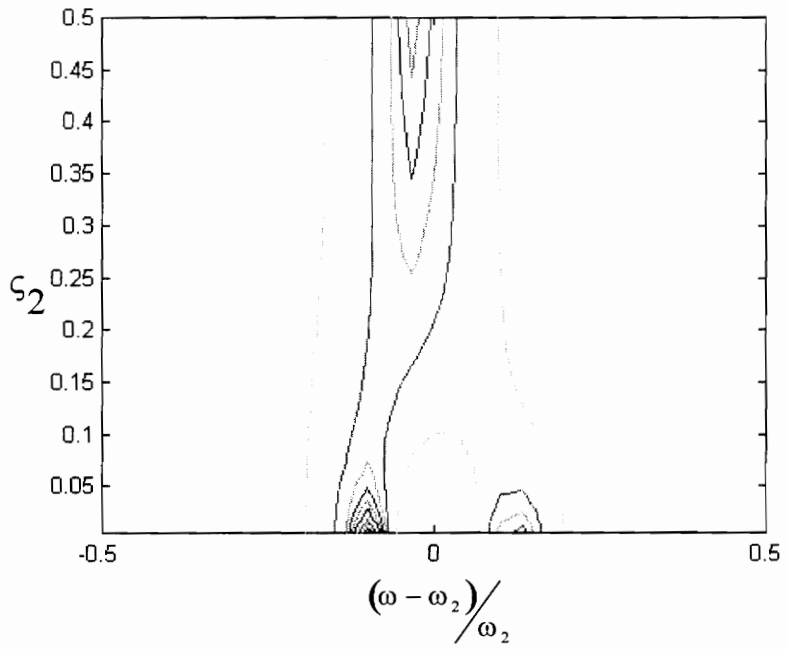

Contour

Figure 2.5 (b): Effect of Varying Absorber Damping and Forcing Frequency

forcing frequency coincides with the appropriate natural frequency for any appreciable amount of time.

For a passive absorber the goal is to choose an absorber damping ratio ς_2 between zero, $\varsigma_2 = 0$, and infinity, $\varsigma_2 = \infty$, for which the peak vibration amplitude of the primary structure in the combined system is minimized. From the magnitude and the contour plots, in Fig. (2.5), one can see that the lowest peak amplitudes occur at an absorber damping ratio of 0.15.

This information is important to us, because, our adaptive absorber will tune to the forcing frequency throughout the absorber's adjustable natural frequency. This results in an optimal absorber damping ratio equal to zero, $\varsigma_2 = 0$. This condition will allow the primary structure displacement to obtain the greatest reduction for an absorber tuned to the forcing frequency.

2.1.4 Effect of Damping in the Primary Structure

Figure (2.6) reveals the effect of damping in the primary structure with no absorber damping. Where the primary structure damping ratio ς_1 is defined as

$$\varsigma_1 = \frac{c_1}{2\sqrt{k_1 m_1}}. \qquad 2.10$$

Both the magnitude and contour plots reveal that increasing the damping ratio of the primary structure decreases the vibration amplitudes at the two natural frequencies. However, increasing primary structure damping ratio also increases the force transmitted to the base or frame. The equation for steady state transmitted force F_t to the base or frame of the system is (James *et al.*, 1989)

$$|F_t| = k_1\sqrt{1+\frac{\omega^2 c_1^2}{k_1^2}}|X_1|. \qquad 2.11$$

From Eq. (2.11), as damping of the primary structure c_1 increases the force transmitted F_t increases also (James *et al.*, 1989). For some applications, e.g. an automobile engine mounted on the frame of the vehicle with an engine mount isolator, this condition is undesirable. The increased force transmitted usually correlates with interior noise in the vehicle, an unpleasant quality to customers. This information is important to us, since, increased damping limits the displacement X_1 of the primary structure. For our primary structure we want the lowest damping possible. The low damping will allow us to obtain the greatest vibration amplitudes for the primary structure when in resonance without an absorber. The larger primary structure vibration amplitudes is desirable to obtain the

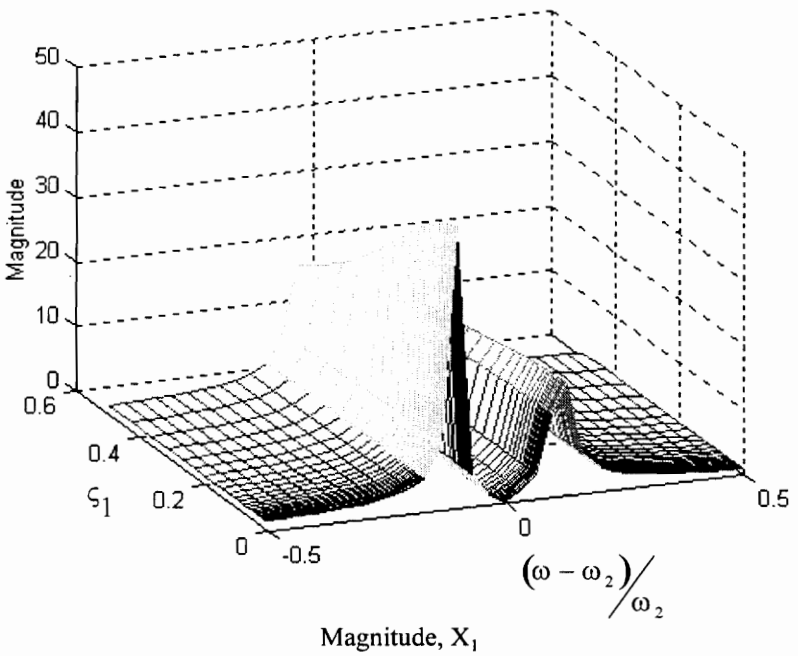

Figure 2.6 (a): Effect of Varying Primary Structure Damping and Forcing Frequency

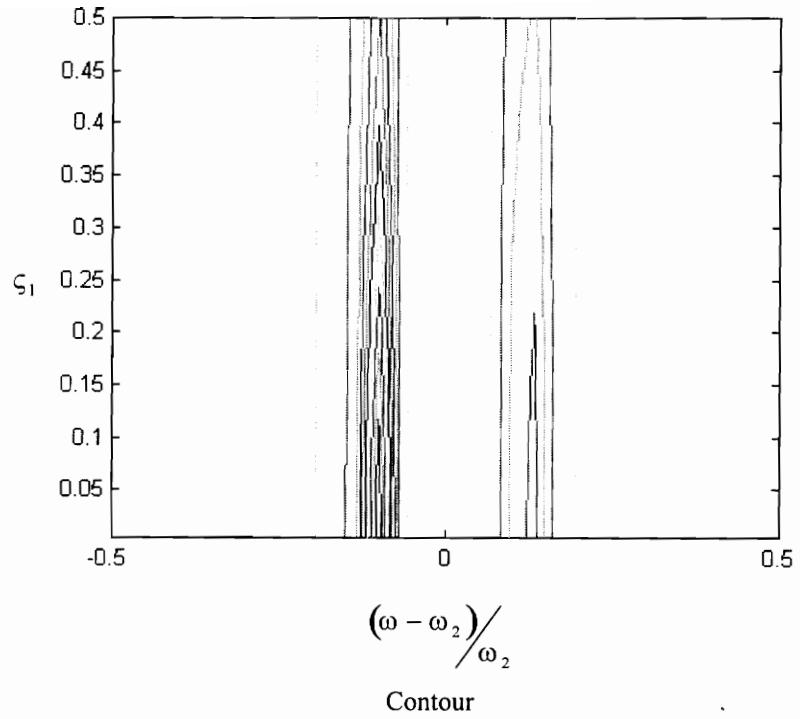

Figure 2.6 (b): Effect of Varying Primary Structure Damping and Forcing Frequency

greatest change in primary structure vibration amplitudes when the absorber is applied to the primary structure.

In summary, an increase in mass ratio will cause the two natural frequencies to become farther apart. When the absorber's natural frequency is below the natural frequency of the primary structure the resulting two natural frequencies are lower than the condition where the absorber and primary structure are tuned to the same natural frequency. Similarly, when the absorber is tuned above the primary structure the resulting two natural frequencies are higher than the condition where the absorber and primary structure are tuned to the same natural frequency. When the absorber natural frequency and forcing frequency are in tune with each other, $\omega_2 = \omega$, and there is no damping in the absorber then the vibration amplitude of the primary structure is equal to zero. By increasing dampingin the absorber, the amplitude of the primary structure increases at the original

natural frequency of the absorber. If the damping of the absorber continues to increase, the two degree of freedom system begins to behave as a single degree of freedom system. Finally, an increase in primary structure damping limits the displacement of the primary structure.

2.2 Control

The controls involved in this project involves two sections. The first stage contains the use of a table look-up. The second stage uses a gradient search method. Figure (2.7) shows where both stages of control are located in the programming flow.

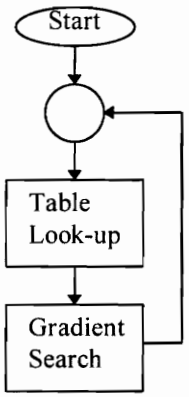

Figure 2.7: Control Flow Chart

2.2.1 Table Look-up

In the table look-up section of the controls, an equation is used to transform a given input into an output. The equation is an approximation between the input and output created from experimental data. This approximation will be shown in Chapter 6 of this thesis.

2.2.2 Gradient Search

The gradient search section searches for the minimum value of a function. The search routine compares two values along the function. Based on the comparison, it continues its

search either in the same direction or the opposite direction. The search routine may or may not change its step size based on the difference between the two values. For our controls we will use a finite step size.

2.3 Summary

In this chapter, we have covered the background information in vibration absorber theory and the control concept used in this project. The absorber theory section presented the effect of an absorber on a primary structure, the effect of the mass ratio on the combined system, and the effects of damping in both the absorber and the primary structure on the combined system. The control concept section presented the table look-up and the gradient search concept.

For the next chapter, Chapter 3, we will present the system description and hardware used throughout the experiments. The structural design of the primary structure, absorber structure, and the combined system are covered.

Chapter 3

3. System Description

In this chapter we will present the system description. The chapter begins with the structural design of the primary structure, absorber structure, and the combined system. Following this section, we will cover the hardware necessary to perform the experiments. Modeling of the system or subsystems is not covered in this thesis. For a description of the modeling please refer to Moyka (1996).

3.1 Structural Design

In this section we present the design of the primary structure, absorber structure, and the combined system. We will present the components of the system relative to each section. We will also present the function as well as the dimensions for certain critical components.

3.1.1 Primary Structure Design

Figure (3.1) shows detail drawings of the side and front views of the primary structure assembly and bottom view of the base. The primary structure consists of an aluminum cantilever beam and attachment hardware for the absorber structure. The aluminum cantilever beam is clamped at ground with a torque force of 3.39 Nm on the two ground clamp bolts. The primary beam has a length of 30.5 cm, a width of 1.27 cm, and a height of 5.08 cm. The attachment hardware for the absorber is located at a distance of 26.0 cm from the clamped end of the beam. The attachment hardware consists of the clearance beam, clamp strip, strip bolts, and the base. The clearance beam allows the absorber structure to be connected to the primary structure without applying clamping force to the threaded rods of the absorber structure. The clearance beam is bolted to the primary

beam with a steel strip and two bolts torqued at 1.13 Nm. This clearance beam has dimensions of 7.62 cm long, 2.54 cm wide, and 0.952 cm deep. Also, the clearance beam contains a vertical hole of 0.635 cm in diam. and 3.17 cm deep so that the threaded rod of the absorber can slide in and out of it without contacting the clearance beam. Attached to the bottom of the clearance beam is the base. The base serves as the location where the absorber attaches to the primary structure. The base is 8.25 cm wide, and its height and depth are 1.9 cm each. The base contains two 0.635 cm diam. holes, a third hole drilled and tapped for a 1/4 - 20 UNC rod, and a fourth hole drilled at 0.475 cm diam. The 0.475 cm diam. hole is for housing the displacement sensor. The threaded hole is for the threaded rod of the absorber. Finally, the remaining two 0.635 cm diam. holes are for the guide rods of the absorber.

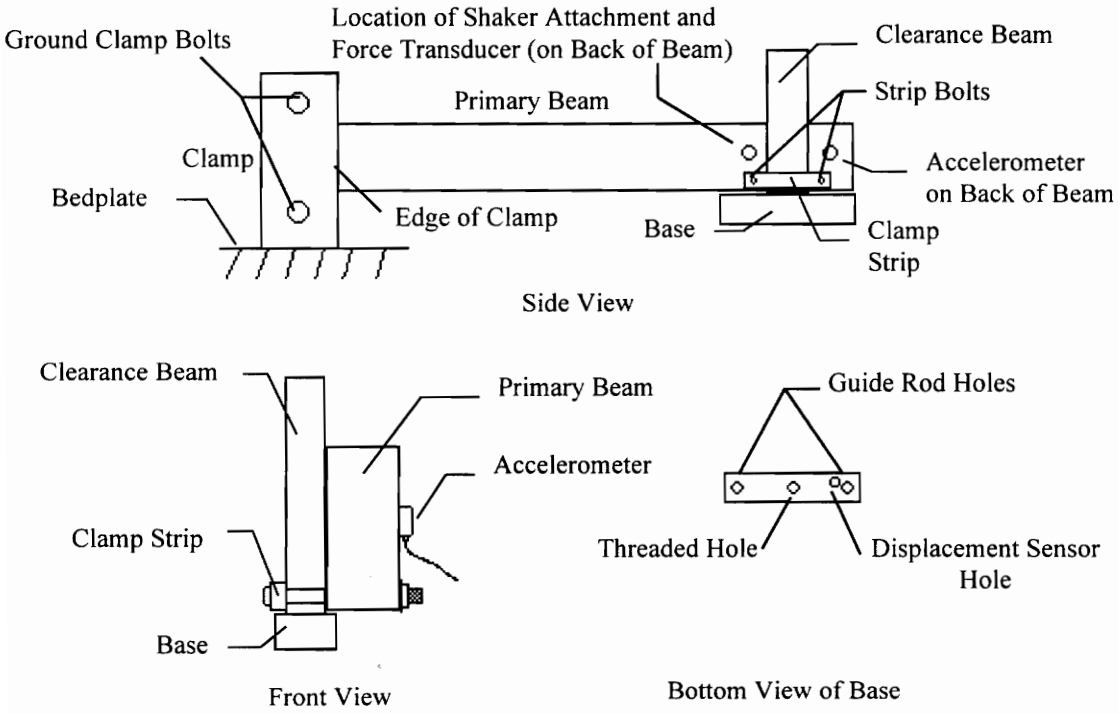

Figure 3.1: Design of Primary Structure

3.1.2 Absorber Structure Design

Figure (3.2) shows detail drawings of the absorber assembly. The absorber structure consists of two steel guiding rods, a steel threaded rod , a coupler, and a stepper motor. The two guiding rods, 0.635 cm diam., are screwed onto the flange of the motor. The threaded rod, 1/4 - 20 UNC, is connected to the shaft of the motor with a coupler.

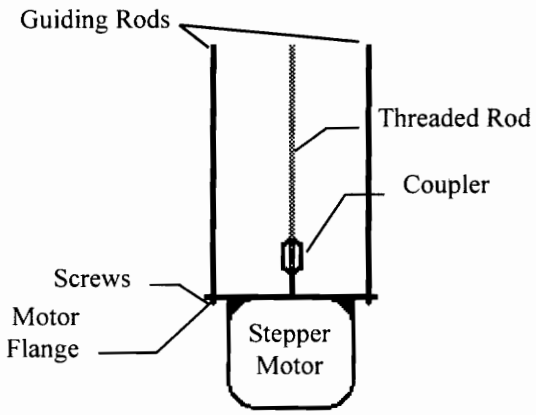

Figure 3.2: Design of Absorber Structure

3.1.3 Combined System Design

Figure (3.3) shows a detail drawing of the combined system. The combined system consists of the primary structure and the absorber structure. The absorber structure is attached to the primary structure at the base's threaded hole with the absorber's threaded rod. The threaded rod screws in and out of the base as the shaft of the motor turns. The absorber's length is adjusted by the motor shaft turning. The absorber is also restrained by the primary structure at the two guide holes. The guide holes and guide rods restrain the motor housing from rotating as the motor shaft turns.

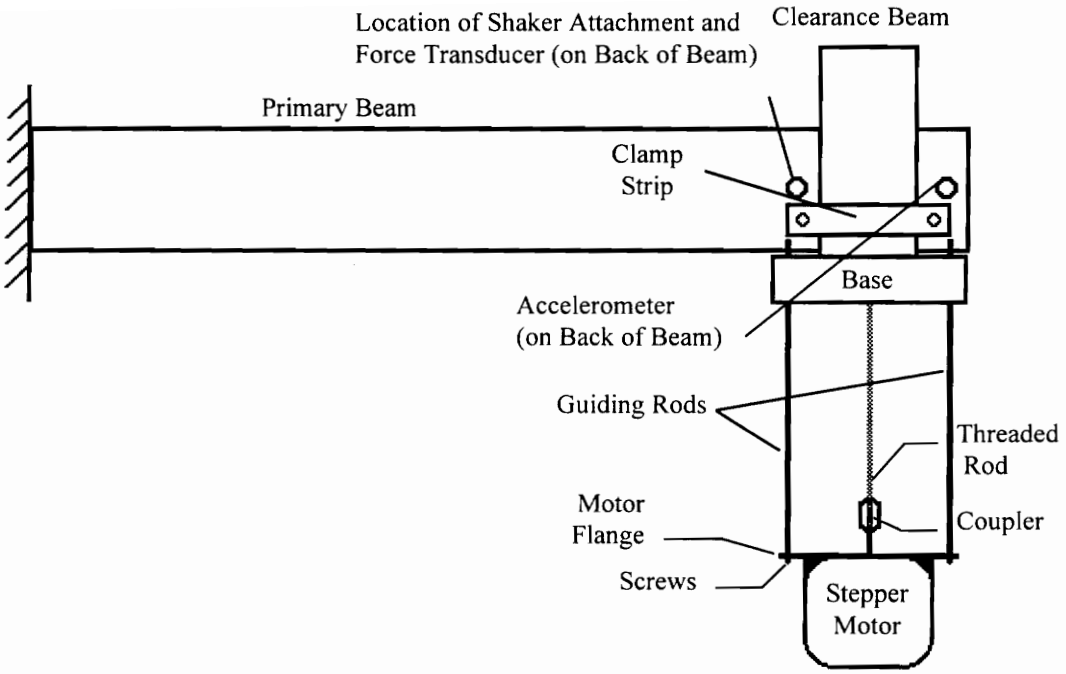

Figure 3.3: Design of Combined System

3.2 Hardware Description

In this section we present the hardware parts of the control system.

3.2.1 Stepper Motor

A 2 phase bipolar stepper motor (Sigma Instruments, Inc.) is used to change the overall length of the absorber structure. The stepper motor is powered and driven by a miniature high performance microstepper called the Panther LI2 (Intelligent Motion Systems). The motor has four leads, each wire is connected to the Panther LI2 at a corresponding pin assignment of connector P1.

3.2.2 Controller/Indexer

The Panther LI2 has all the components necessary to drive a motor integrated into one piece of hardware. The Panther LI2 contains the microstep driver, indexer and power supply.

The indexer communicates at a 9600 Baud rate using the RS-422 protocol. The line settings are: data length (8), stop bits (1), and parity (none). The Panther LI2 has a built in RS232 to RS422/485 converter. The Panther LI2 has its own language and parameters. A sequence of ASCII characters written to the Panther LI2 are used to initialize the Panther LI2 and to control the stepper motor. Some of the Panther's capabilities are programmable trip position, programmable initial and final velocities of the motor, programmable speeds (steps per second), step resolution and direction. Step motion is controlled at speeds up to 20,000 steps per second. Furthermore, stepper motor position and the ramp slope for the motor speed can be controlled. Table (3.1) is a list of parameters and their standard defaults to command the Panther LI2.. These parameters are stored and recovered as a set when the Panther LI2 is turned on. These parameters can be changed by sending the appropriate ASCII command characters to the Panther L12.

Table 3. 1: Panther L12 Parameters and their Standard Defaults

Parameters	Standard Defaults
Initial velocity (I)	400 steps per second
Slew velocity (V)	3004 steps per second
Divide factor (D)	0 (Full Step)
Ramp slope (K)	10/10
Jog speeds (B)	30,200
Trip point (T)	off
Step Resolution (H)	1 (Auto Variable)
Auto power down	yes
Hold/Run current	5/25
Limit polarity	low
Auto position readout (Z)	off
Name (after reset)	undefined

Table (3.2) contains the commands used for the control programs. For a more descriptive definition refer to instrumentation literature.

Table 3. 2: Panther L12 Commands Used for Control

Common Commands	Function
M	Move at Fixed Velocity
O	Set Origin
R	Relative Index
V	Set Slew (Final) Velocity
Z	Read Position
±	± Index

3.2.3 Philtec Displacement Sensor

A fiber optic displacement sensor (Philtec, Inc.) is used to determine the home position of the absorber stepper motor. The sensor is powered by a DC power source of +9 to +30 Volts. Any suitable voltage readout device can be connected to the output terminals of the sensor. The sensor is mounted perpendicular to the motor flange. The sensor can be adjusted in and out from the target surface to obtain the largest voltage readout. Next, the gain can be changed to make the peak voltage equal to 5.00 Volts. We were only concerned with maintaining the same reference point, so we used the current gain setting of the sensor and did not recalibrate the sensor.

3.2.4 All Components

Table (3.3) is a list of all the hardware components used to conduct the experiments.

Table 3. 3: Hardware Used for Control

Instrument	Make	Model #	Serial #
DC Power Supply	Hewlett Packard	6200B	N/A
DC Power Supply	Hewlett Packard	6296A	N/A
Microstepper Driver, Indexer and Power Supply	Intelligent Motion Systems Inc.	Panther LI2	59006
Oscilloscope	JDR Instruments	3500	3511008
Accelerometer	Kistler Instruments	8630A50	C84579
Force Transducer	Kistler Instruments	9712A50	C45540
Impulse Force Hammer	Kistler Instruments	9724A2000	C44053
Piezotron Coupler	Kistler Instruments	5112	N/A
Shaker	Ling Dynamic Systems LTD	200	892071
Quadra 700 Computer	Macintosh	M5920	F1241HLLC82
Digital Multimeter	Micronta	22-194	N/A
A/D Board	National Instruments	Lab-NB	180805-01
Displacement Sensor	Philtec, Inc.	88NE3	274
20 Watt P.A. Amplifier	Realistic	MPA-25	2A88
Stepper Motor	Sigma Instruments Inc.	20-2215D-28185	N/A
Fourier Analyzer	Tektronix	2630	B010370
Voltage Controlled Generator	Wavetek	VCG III	129758
PC Computer	WIN Laboratories LTD	AT 386	AT91066801

3.3 Summary

In this chapter, we have presented the system description. We first presented the structural design of the primary structure, followed by the design of the absorber structure and the design of the combined system. Following this section, we covered the hardware necessary to perform the experiments.

For the next chapter, Chapter 4, we will present the control program, LabView. We will cover the initialization process for the absorber structure and the main program for control of the absorber structure.

Chapter 4

4. LabView

In this chapter we will present the control program LabView. The chapter begins with a description of the initialization process for the absorber structure on the combined system. We will cover the main program for controlling the absorber structure on the combined system. In the main program we will present the table look-up portion of the control program and the gradient search portion of the control program

4.1 Initialization

In this section we will present the LabView Virtual Instruments (VI's) used to initialize the controller/indexer and to set the absorber motor home position. Figure (4.1(a)-(b)) shows the initialization VI program used to initialize the system and set the absorber motor position.

Figure (4.1(a)) shows a for loop that will execute seven times beginning with zero. Wired to the counter is a case structure. The case structure will implement the internal program for each frame based on the value of the counter. The first frame executed is the case structure with the value of zero in the header. The first frame sends a "space" to the serial communication VI. The serial communication VI will be discussed later in this chapter. Using the option '\' **Codes Display** for the string indicator, LabView will interpret the characters immediately following a backslash as a code for non-displayable characters. The serial communication VI forwards the command to the controller/indexer. The controller/indexer responds with a sign on message.

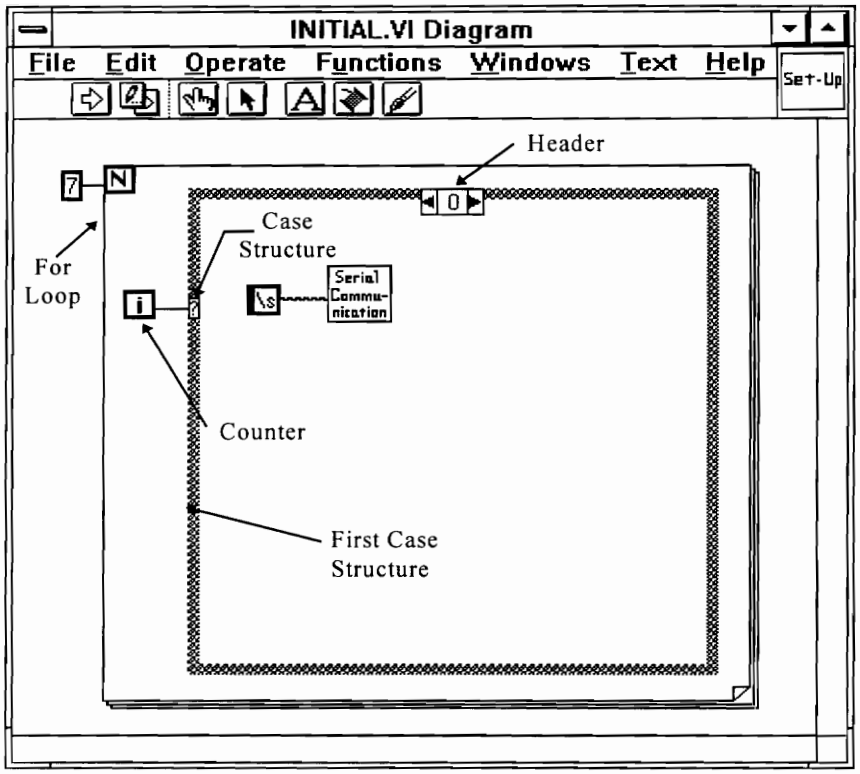

Figure 4.1(a): VI for Initializing the Controller/Indexer and Setting Motor Home Position

Figure (4.1(b)) shows the remaining case structures for the set-up VI. The second case structure sends a "return" to the serial communication VI and waits one second while the controller/indexer responds. The "return" command sets the controller/indexer so that it can begin accepting commands. The third case structure sets the slew velocity of the absorber motor to 1000 steps per second. The fourth case structure implements a while loop. The while loop will continue to implement until the voltage from channel two of the A/D board becomes larger than 1.14 Volts or is less than 0 Volts. This voltage corresponds to the voltage output of the displacement sensor. The sensor maximum voltage can be adjusted by the user by changing the gain of the sensor. Refer to displacement sensor documentation for further information. As long as the conditions for the while loop are met, the program will step the absorber motor in the positive direction at 100 steps per iteration. Once either of the conditions of the while loop are not

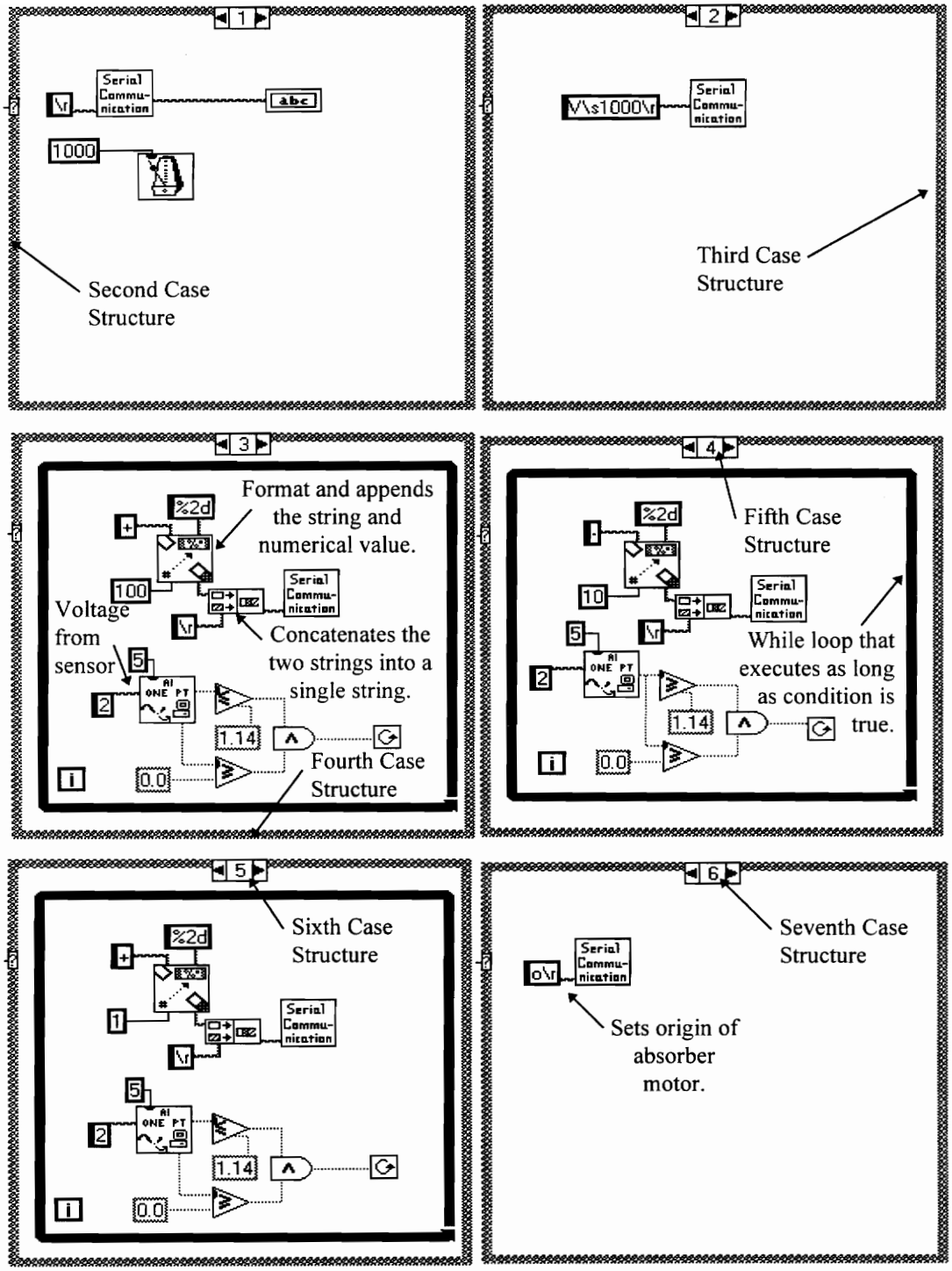

Figure 4.1(b): VI for Initializing the Controller/Indexer and Setting Motor Home Position

satisfied, the loop stops and the fifth case structure begins. This case structure implements a while loop, also. The while loop will continue to implement until the voltage from the displacement sensor becomes less than 1.14 Volts. As long as this condition for the while loop is met, the program will step the absorber motor in the negative direction at 10 steps per iteration. Once this condition of the while loop is not satisfied, the loop stops and the sixth case structure begins. This case structure implements another while loop. This while loop will continue to implement until the voltage from the displacement sensor becomes larger than 1.14 Volts or is less than 0 Volts. As long as the conditions for the while loop are met, the program will step the absorber motor in the positive direction at 1 step per iteration. Once either of the conditions of the while loop are not satisfied, the loop stops and the seventh case structure begins. This case structure sends a command to the controller/indexer to set this position of the absorber motor as the home position.

In the next section, we will present the main program for controlling the absorber natural frequency. Recall from Chapter 3 that the natural frequency of the absorber corresponds to the absorber motor position and, as will be presented in Chapter 5, the absorber motor position is also related to the input voltage controlling the forcing frequency.

4.2 Main Program

In this section, we will present the VI's used in the main program for controlling the absorber natural frequency. First we will present the general flow of the main program. Next we will present the main program front panel and back panel. Then, we will present the portion of the control program responsible for the table look-up. Lastly, we will present the portion of the control program responsible for the gradient search .

Figure (4.2) shows the control flow for the main program. The program contains two important sections. The first section is the table look-up. This section tunes the absorber

natural frequency very near the forcing frequency. The second section is the gradient search. This section optimizes the absorber natural frequency by tuning it to match the forcing frequency. The program will return from the gradient search section to the table look-up section whenever the forcing frequency changes.

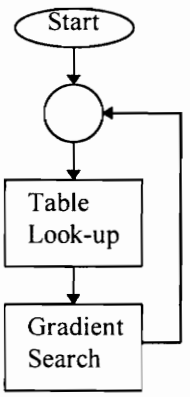

Figure 4.2: Control Flow of Main Program

Figure (4.3(a)) shows the front panel for the MAIN VI. This panel has an on-off switch so that the program can be terminated when it returns to the beginning of the program and the switch is in the off position. The front panel displays the original absorber motor

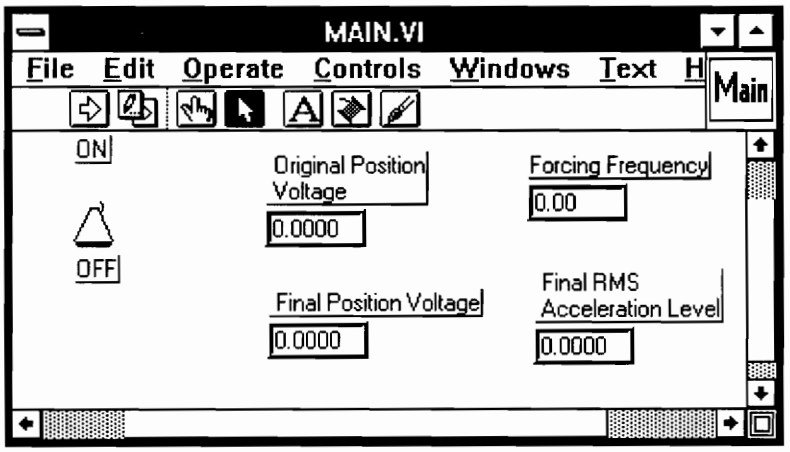

Figure 4.3(a): Front Panel VI for the Main Program.

position voltage (input voltage), forcing frequency, final absorber motor position voltage, and final rms acceleration level. When the program returns from the optimization routine (gradient search) and the on-off switch is turned off, the program will terminate and the user can look at the display to see the final absorber motor position voltage and the final rms acceleration level of the primary structure.

Figure (4.3(b)) shows the back panel for the MAIN VI. The MAIN VI begins by reading the input voltage, which is related to the forcing frequency (as will be discussed in Chapter 5), and the absorber motor position. After the left side shift register receives the input voltage value, the program begins the first while loop. This loop will continue executing as long as the Boolean switch on the front panel is in the on position. The left side shift register reads the input voltage value for the first loop. For all remaining loops, the left side shift register receives the voltage value from the right side shift register of the previous loop. This allows information to pass from one execution to the next. After entering the first while loop, the program enters the second while loop and passes the input voltage value to the second while loop's left side shift register. The second while loop is also the table look-up portion of the main program. Once the conditions are not met for the second while loop, the program flow passes the voltage value from the second while loop right side shift register to the sequence structure. The sequence structure implements each frame in order beginning with frame zero. Frame zero contains the gradient search routine. When the gradient search routine is done implementing, the program will execute frames one and two. Frame one is a half second delay and frame two obtains a new input voltage to pass to the right side shift register of the first while loop. The input voltage value then goes to the left side shift register and begins the table look-up again.

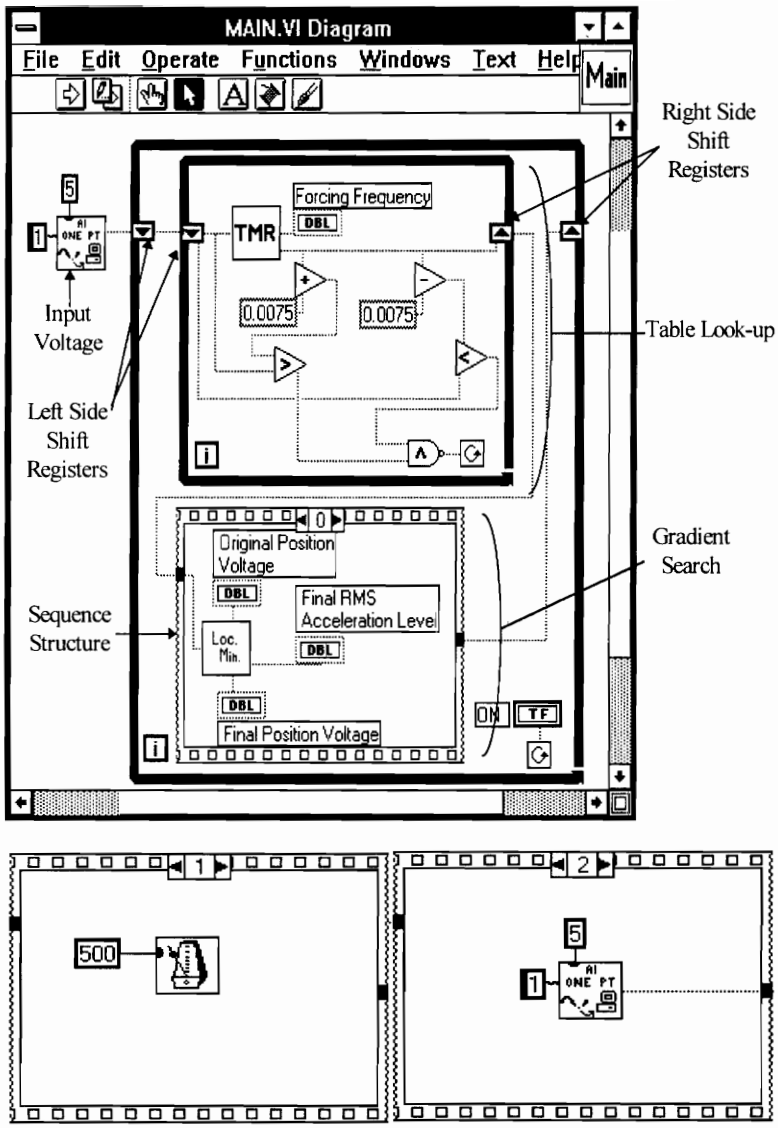

Figure 4.3(b): Back Panel VI for the Main Program

The next section will present the table look-up portion of the main program and any sub VI's used for the table look-up.

4.2.1 Table Look-up

Figure (4.4) shows the detail programming flow for the table look-up. The table look-up is used in the initial process of moving the absorber motor to the proper location for the

original forcing frequency detected or for a newly changed forcing frequency. The table look-up converts the input voltage, which is proportional to the forcing frequency, to a particular motor position value, which is directly related to the absorber natural frequency. The motor position value is sent to the controller/indexer which in turn sends a command to the motor to go to the proper motor position. Once the controller/indexer command for motor position is sent, the controls detects the input voltage again. If the input voltage (referred to as forcing frequency) changes then the controls will reimplement the table look-up. Once the absorber motor is at the proper location and if the forcing frequency does not change then the gradient search, which will be discussed later in this chapter, is automatically implemented to optimally tune the natural frequency of the absorber to the forcing frequency by adjusting the absorber motor position.

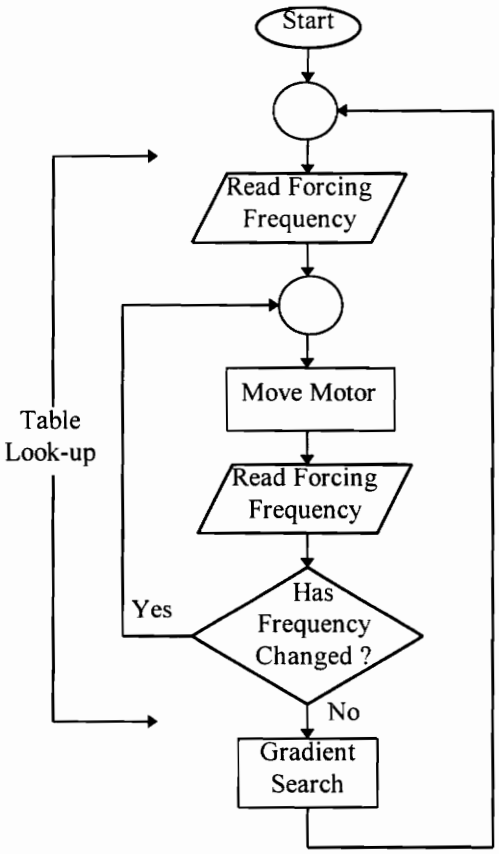

Figure 4.4: Table Look-up Flow Chart

Figure (4.5) shows the LabView table look-up portion of the MAIN VI. This portion of the MAIN VI begins when an input voltage value is passed to the left side shift register. The table look-up continues to implement as long as the value at the left side shift register is either greater than or less than the outputted value from the TMR VI by 0.0075 units. The TMR VI transforms the input voltage value to an absorber motor position and sends commands to move the absorber motor to this new position. The TMR VI then reads a new input voltage from the input source and passes the value back to the MAIN VI. The TMR VI will be presented later in this chapter.

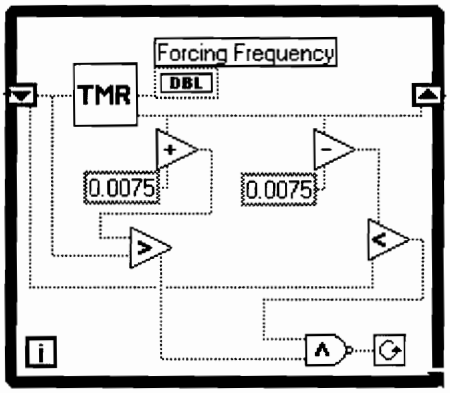

Figure 4.5: Table Look-up Portion of MAIN VI

4.2.1.1 Transform Move and Read (TMR) VI

Figure (4.6) shows the TMR VI diagram. The TMR VI implements 3 frames of a sequence structure. The first slide transforms the input voltage value from the digital indicator to the related forcing frequency value and transforms the input voltage value to a motor position to be sent to the controller/indexer. Based on the comparison of the control voltage values and the input voltage values the greater than or equals and the less than or equals logic operators will give a true or false statement. These statements will determine whether the respective following true/false case structures will implement a true or false case structure. Based on the true/false case structures, the input voltage value is either passed unchanged or changed to another value. The control voltage values are

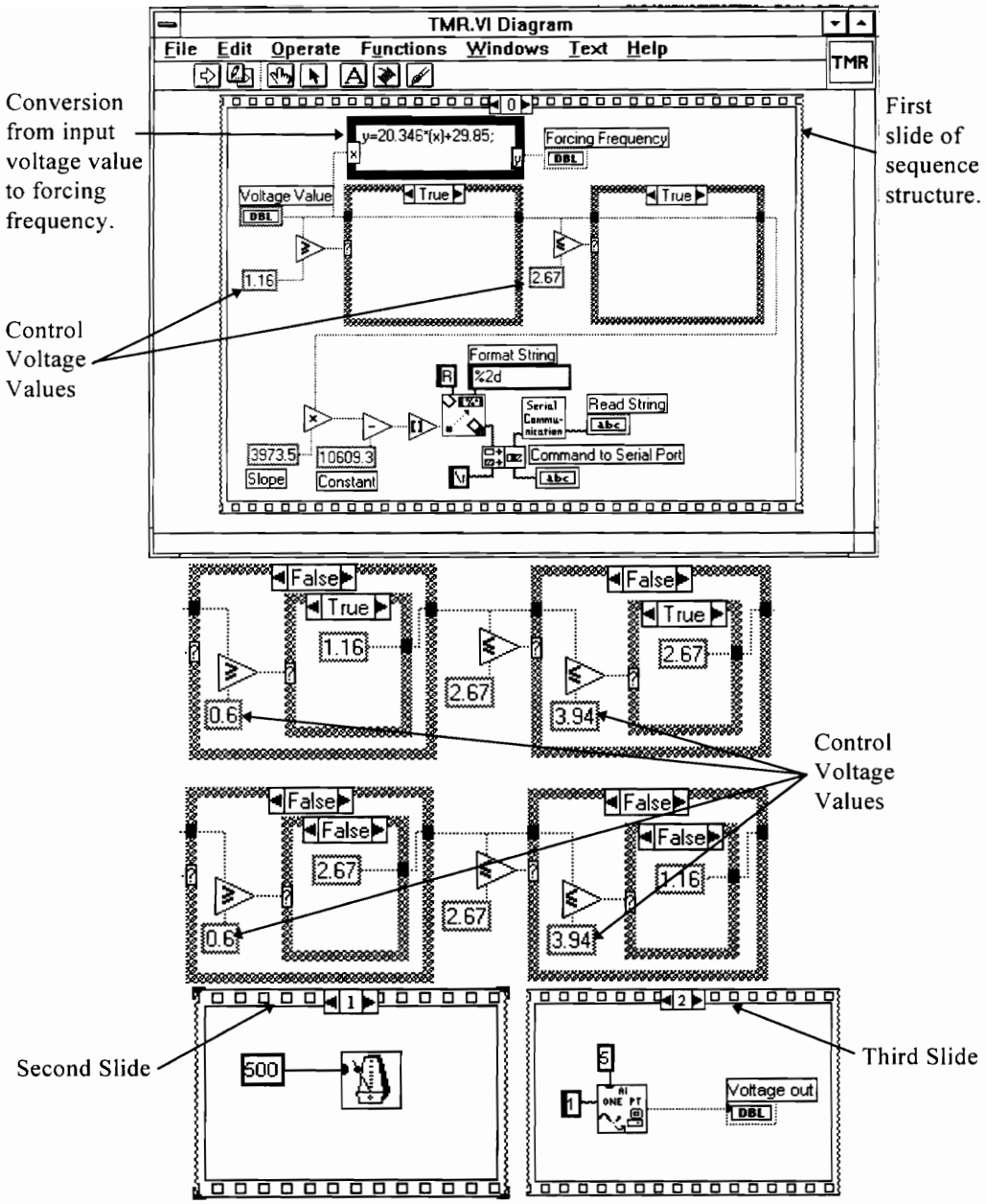

Figure 4.6: Transform Move and Read VI for the Main Program

determined based on at which forcing frequencies the absorber's natural frequency is to be adjusted from the highest of the absorber frequency range to the lowest of the absorber frequency range and vice versa. The control voltage values also control at what range of frequencies the absorber is to track the forcing frequency. In the second slide the VI waits

for half a second and then goes to the third slide. The third slide reads a new input voltage to be sent to the front panel and/or the calling program.

4.2.1.2 Serial Communication (SER) VI

Figure (4.7) shows the SER VI diagram. The SER VI initializes the serial port based on

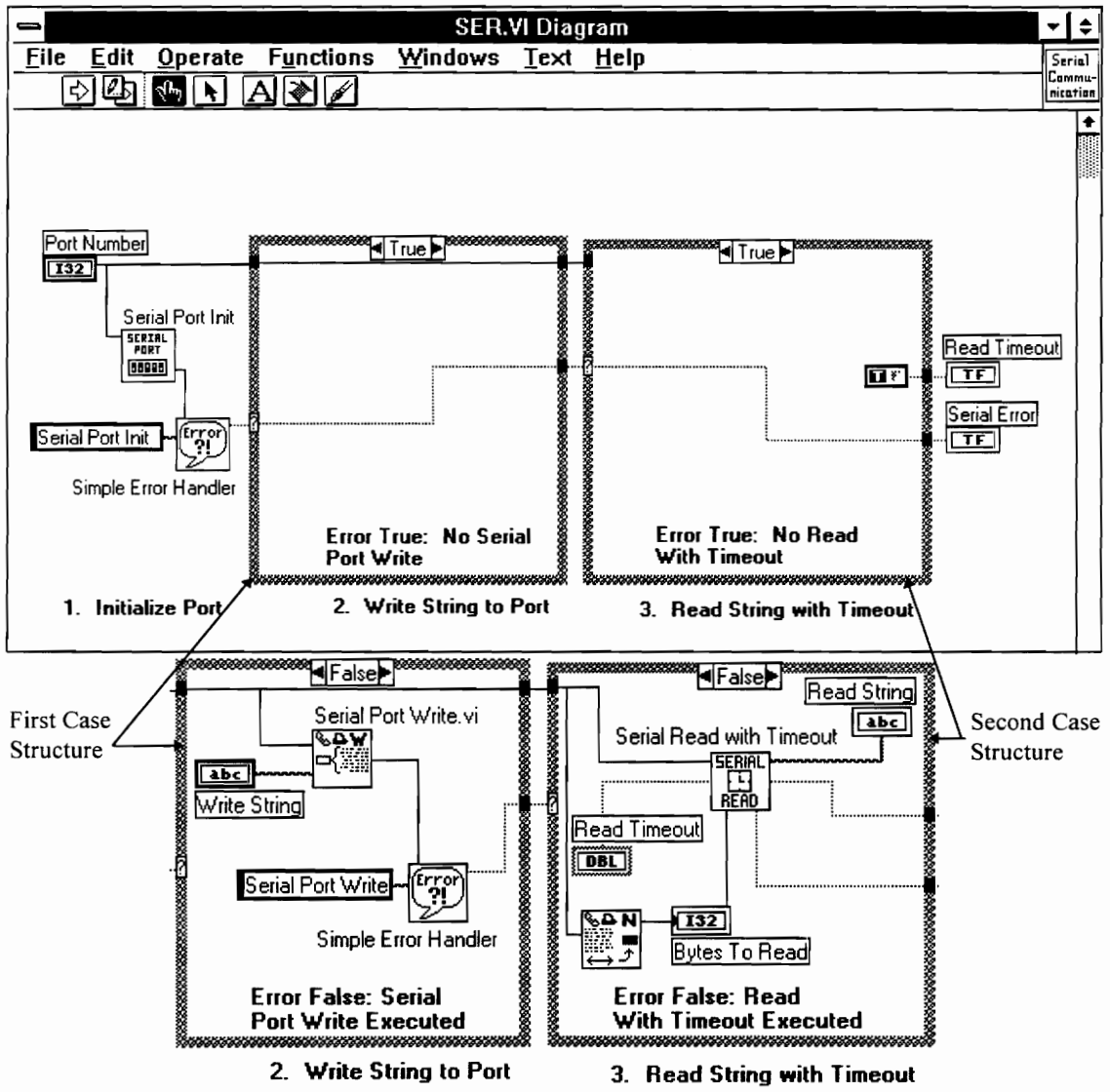

Figure 4.7: Serial Communication VI

the port number transferred to the SER VI from the front panel and/or calling program. If there is an error in the initialization, the error handler will give a true statement and implement the first and second true case structures; therefore, the SER VI will respond with a serial error. However, if the initialization is successful the error handler will give a false statement and implement the first false case structure. The first false case structure takes the write string from the front panel and/or calling program and sends it to the serial port. If this is not a successful operation then the serial-port-write error handler gives a true statement to be used by the second case structure. The true statement will implement the second true case structure, which will result in a serial error. If the write string is successfully sent to the serial port, the error handler gives a false statement for the second true/false case structure. The second false case structure reads bytes from the serial port based on the Bytes to Read Value. If the read string does not receive at least the proper number of bytes before the Serial Read with Timeout has timed out then a read timeout error will occur. If the read string receives the proper number or more of bytes from the serial port then no timeout error will occur. Additional bytes received in addition to the required number of bytes to read are truncated. The SER VI sends the bytes to the readstring and returns to the program that called the SER VI or ceases execution.

4.2.2 Gradient Search

The gradient search is the process of stepping the motor in one direction and comparing acceleration levels for the two positions and deciding whether or not to continue to step in that direction. This method is used because it is simple to implement and requires only one input to be monitored for the search. Once the forcing frequency reaches a steady state value in the table look-up section, the program for the controls begins the gradient search routine (See Fig. (4.8)). In Fig(4.8) a counter value is represented by (I) and the absorber motor position value is determined by (P). The acceleration level of the primary structure is determined for the original absorber motor location. Then the absorber motor

is stepped in a predetermined direction and step size, therefore changing the absorber's natural frequency. The acceleration level is determined for this new absorber motor position. If the acceleration level increases, then the absorber motor will step in the opposite direction and the acceleration levels between the original absorber motor position and the new absorber motor position are compared. Based on the comparable acceleration levels of the absorber motor's first step in the opposite direction and the absorber motor at its original position, the absorber motor will continue to step in the opposite direction or the motor will return to its original position. If the acceleration levels of the primary structure are lowest at the absorber motor original position then the absorber motor returns to the original position, otherwise the absorber motor continues to step in the opposite direction. For each iterative step a comparison of acceleration levels is made between the new absorber motor position and the previous absorber motor position. If the acceleration decreases as the absorber motor steps in either the original direction or the opposite direction, then the absorber motor will continue to step in the appropriate direction until either the acceleration level increases or the highest or lowest position of the absorber motor is reached. If there is an increase in acceleration during the stepping process then the absorber motor will return to the previous step and remain there. If the absorber motor reaches the highest or lowest position of the absorber motor's range before an increase in the acceleration level then the absorber motor will stay at this highest or lowest position. Throughout points of the gradient search process a check is completed to see if the forcing frequency has changed. If a forcing frequency change has occurred then the gradient search routine ceases and programming flow returns to the beginning of the table look-up routine.

Upon completion of the gradient search routine, the control system monitors for changes in the forcing frequency. If the forcing frequency changes then the controls will implement the table look-up. If the forcing frequency continues to change then the

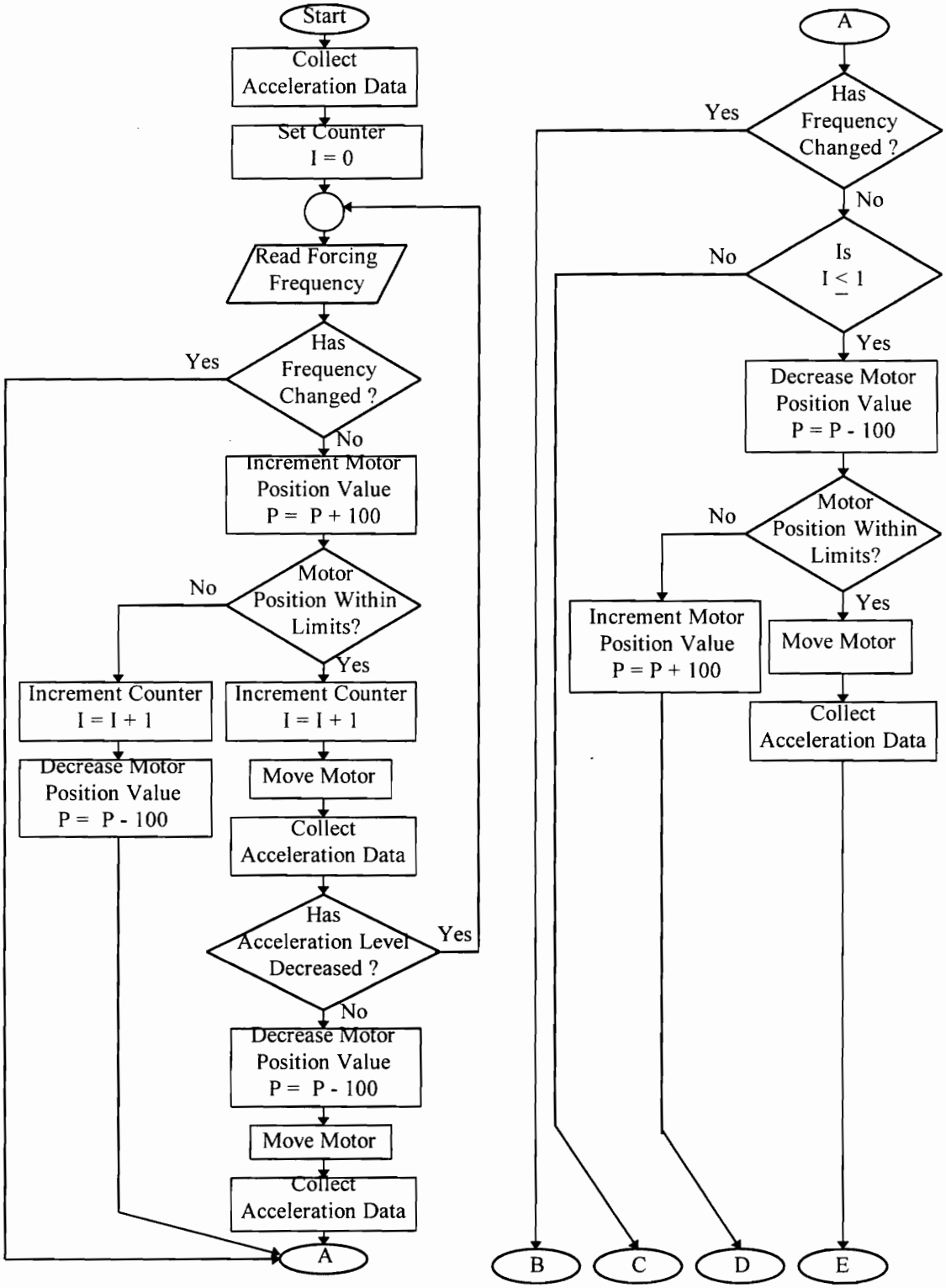

Figure 4.8(a): Program Flow for Gradient Search of Main Program

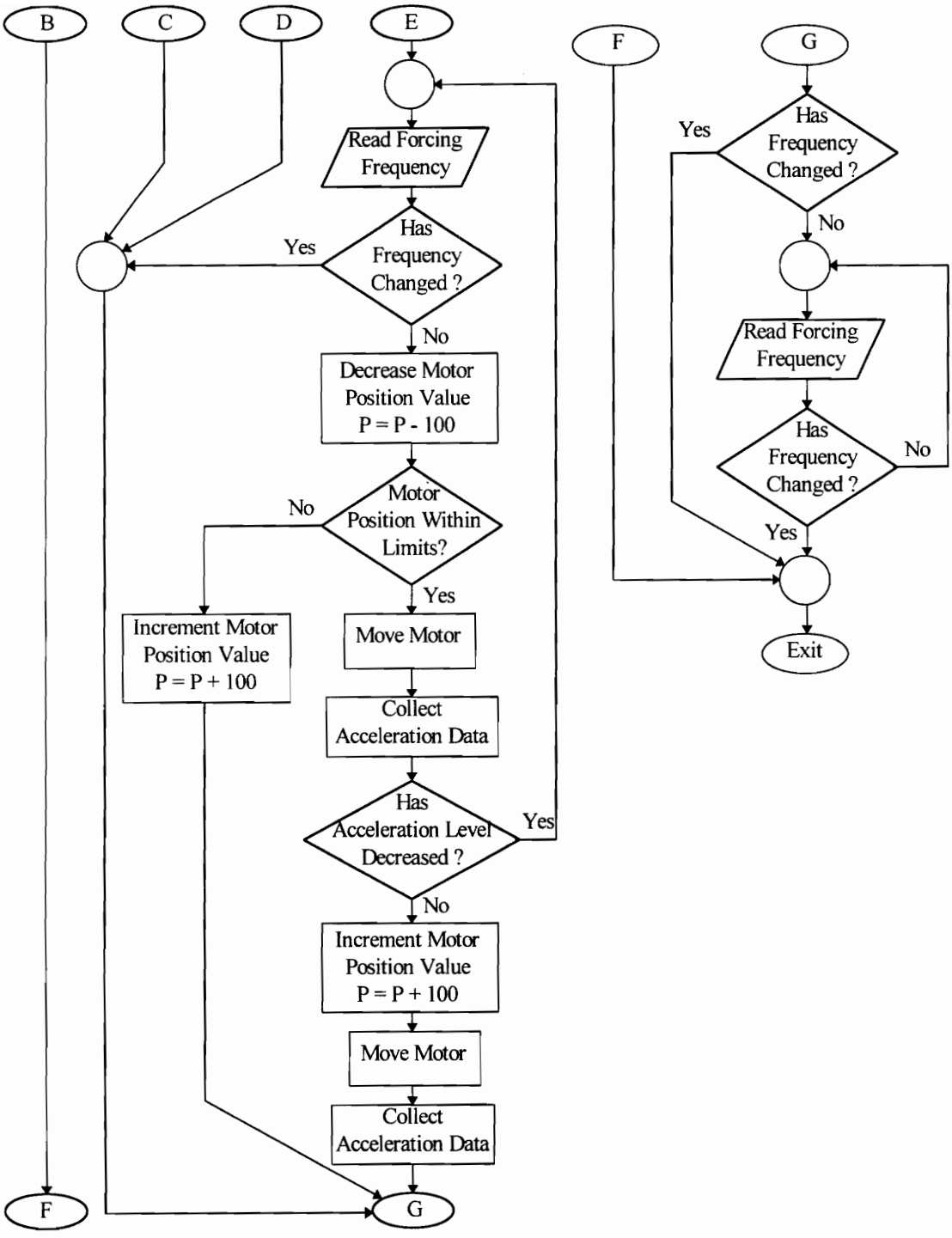

Figure 4.8(b): Program Flow for Gradient Search of Main Program

controls will re-implement the table look-up again. Finally, if the forcing frequency does not change then the gradient search method will be reimplemented.

Figure 4.9 shows the first portion of the gradient search routine (LOC_MIN VI). The LOC_MIN VI uses a while loop with several true/false case structures as well as some sequence case structures. The LOC_MIN VI receives an input voltage value from the main program that corresponds to the forcing frequency and the original absorber motor location. This voltage value is sent to two left side shift registers of the while loop. This voltage value is used throughout the gradient search routine to determine if the forcing frequency changes. The rms acceleration level is determined for the original absorber motor location using the collect data VI (cd VI) and sent to the left side shift register for the while loop. The cd VI will be discussed later in this chapter. The counter value is set to zero and sent to the left side shift register of the while loop. Once all the information has reached the while loop, the VC VI compares a new input voltage value with the original input voltage value received from the main program and the left side shift register. The VC VI will be discussed later in this chapter. If there has been a value change, the VC VI will respond with a false statement. This false statement will result in the first true/false case structure implementing its false case structure and will cause the while loop to cease execution upon the completion of the false case structure. The false case structure will pass the most recent rms. acceleration levels of the primary structure, voltage value representing the absorber motor position, and counter value to the second portion of the gradient search routine (Loc_min2 VI). The Loc_min2 VI will also receive the original voltage value for the forcing frequency as well as the true/false statement from the VC VI. If there has not been a voltage change, the VC VI will respond with a true statement. The true statement will result in the first true/false case structure implementing its true case structure.

The true case structure for the first true/false case structure begins by increasing the voltage value representing the absorber motor position by 0.05 units. Next, the new motor position value is compared with the upper limit and lower limit for the absorber motor position. If the new absorber motor position value is outside the absorber motor position bandwidth then a false statement is sent to the second true/false case structure. The false statement will result in the second true/false case structure implementing its false case structure. If the new absorber motor position value is within the absorber motor position bandwidth then a true statement is sent to the second true/false case structure.

The true case structure for the second true/false case structure uses a sequence structure of three frames to transfer the absorber motor to its new position, collect new rms acceleration levels, and compare the rms acceleration levels of the new absorber motor position with the previous absorber position. If the acceleration values of the new absorber motor position decrease then a true statement is sent to the third true/false case structure and the operator for the while loop, otherwise a false statement is sent. The second true/false case structure, regardless if it is the true or false case structure, also increases the counter value by one each time it is implemented. The false case structure for the second true/false case structure decreases the motor position value by 0.05 units, back to its previous value.

The true case structure for the third true/false case structure passes along the rms acceleration value received and the most recent absorber motor position value. The false case structure for the third true/false case structure uses a sequence structure of three frames to reduce the absorber motor position value by 0.05 units, move the absorber motor to the new absorber motor position value, and collect the rms acceleration level at this new absorber motor position. The new absorber motor position value and rms acceleration value are passed on to the next operation.

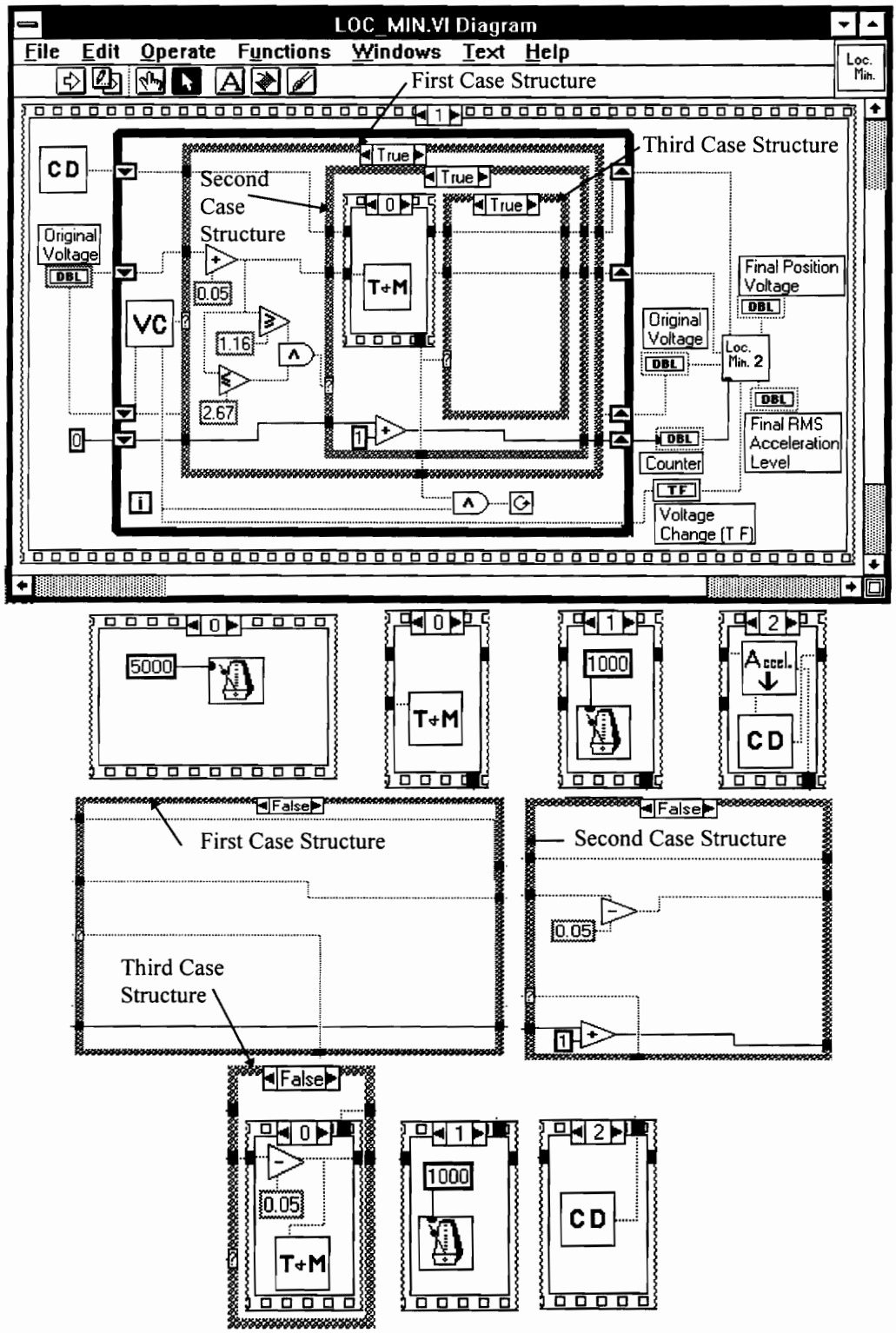

Figure 4.9: Locate Minimum VI

Upon completion of the true/false case structures and the sequence structures, the most recent rms acceleration values, absorber motor position value, original forcing frequency value, and the increment counter value are sent to the right side shift register of the while loop. As long as the while loop receives true statements and continues to run, the right side shift register values are sent to the left side shift register for the next loop. If the while loop receives a false statement and ceases to run, the right side shift register values are forwarded to the next receiving operations. When the while loop ceases execution the original forcing frequency value, counter value, absorber motor position value, the true or false statement from the VC VI, and the most recent rms acceleration value are sent to the next section of the gradient search routine (Loc_min2 VI). Loc_min2 VI will be discussed later in this chapter. After Loc_min2 VI is completed the final rms acceleration value and the final absorber motor position value are sent to the front panel of the Loc_min VI and/or to the calling program.

4.2.2.1 Collect Data (CD) VI

Figure (4.10) shows the cd VI diagram. The cd VI implements an analog input multipoint VI from the functions toolbox of LabView to collect 12,500 acceleration values at 12,500

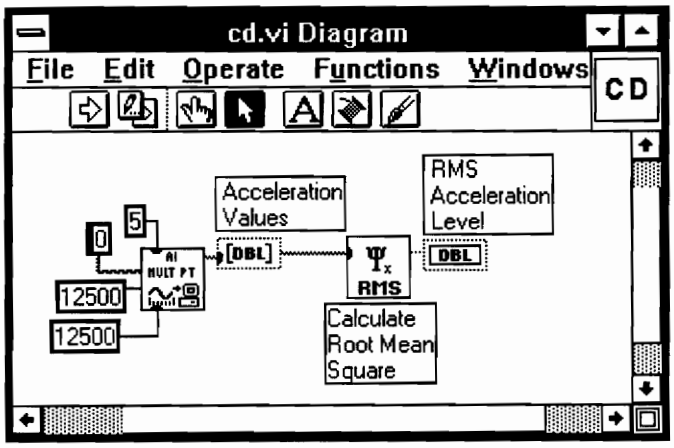

Figure 4.10: Collect Data VI

samples per second. The acceleration values are passed to an array for storage. A RMS VI from the functions toolbox is used to calculate the root mean square (rms) acceleration value from the array of acceleration values. This rms acceleration value is then passed to a front panel readout and/or passed back to the calling program.

4.2.2.2 Voltage Change (VC) VI

Figure (4.11) shows the VC VI diagram. The VC VI implements an analog input one point VI from the functions toolbox of LabView to collect a single voltage value representing the forcing frequency. This value is increased and decreased by a value of 0.02 units. These new values are compared to the original voltage value passed to the VC VI from the calling program and/or front panel. If the new voltage value plus 0.02 units is greater than the original voltage value then the Greater Than logic operator will return a true statement, otherwise if the new voltage value is less than or equal to the original voltage value a false statement will be given. If the new voltage value minus 0.02 units is less than the original voltage value then the Less Than logic operator will return a true statement, otherwise if the new voltage value is greater than or equal to the original voltage value a false statement will be given. An And logic operator is used to compare the true/false statements given from both the Greater Than and Less Than logic operators.

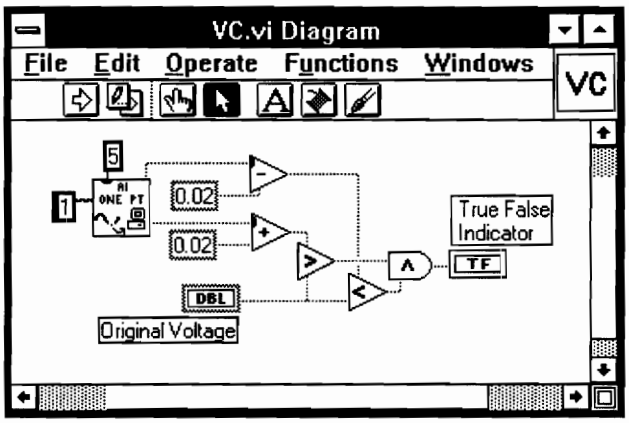

Figure 4.11: Voltage Change VI

If both are true then a true statement is given. If either statement is not true than a false statement is given. The And logic operator true/false statement is passed to the front panel true/false indicator and/or the calling program.

4.2.2.3 Transfer And Move (T&M) VI

Figure (4.12) shows the T&M VI diagram. The T&M VI transforms the input voltage

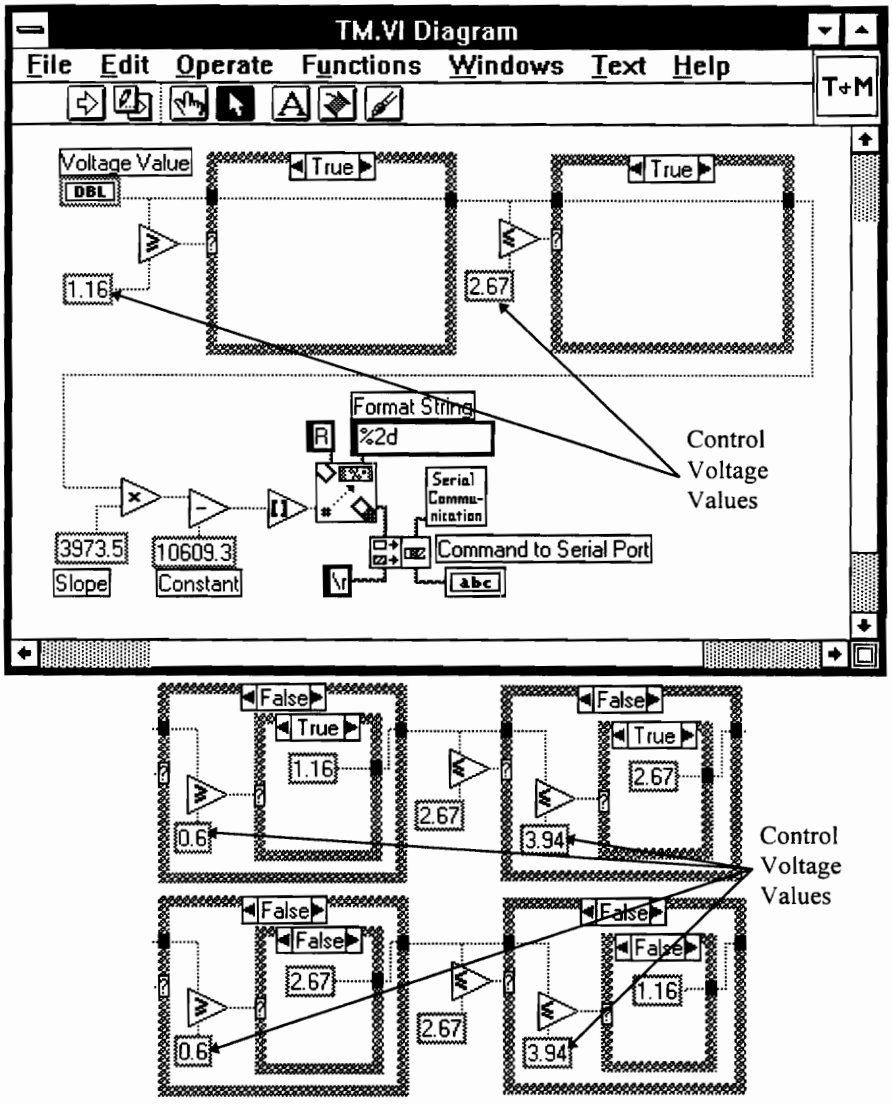

Figure 4.12: Transfer and Move VI

value from the front panel and/or calling program to a motor position to be sent to the controller/indexer. Based on the comparison of the control voltage values to the input voltage value the Greater Than or Equals and the Less Than or Equals logic operators will give a true or false statement. These statements will determine whether the respective following true/false case structures will implement a true or false case structure. Based on the true/false case structures, the input voltage value is either passed through unchanged or changed to another value. The control voltage values are based on at which forcing frequencies the absorber's natural frequency is to be adjusted from the highest of the absorber frequency range to the lowest of the absorber frequency range and vice versa. The control voltages also control at what range of frequencies the absorber is to track the forcing frequency.

4.2.2.4 Compare Acceleration Levels (Accel) VI

Figure (4.13) shows the Accel VI. The Accel VI implements a Less Than operator to determine if the new rms acceleration value is less than the previous rms acceleration value. If the new rms acceleration value is less than the previous rms acceleration value then a true statement is sent to the front panel indicator and/or the calling program.

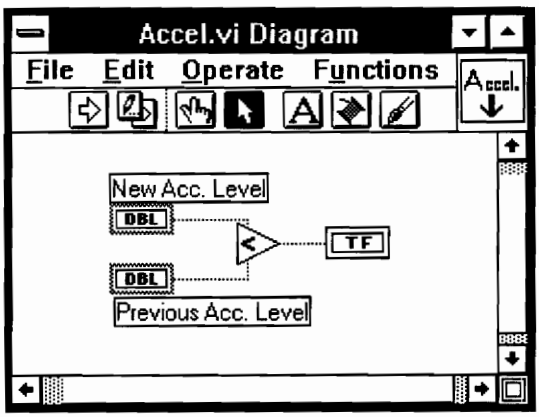

Figure 4.13: Acceleration Comparison VI

4.2.2.5 Locate Minimum Two (Loc_min2) VI

Figure (4.14) shows the Loc_min2 VI. The Loc_min2 VI is a sub VI of Loc_min VI. Both VI's are part of the gradient search routine of the main program. The Loc_min2 VI

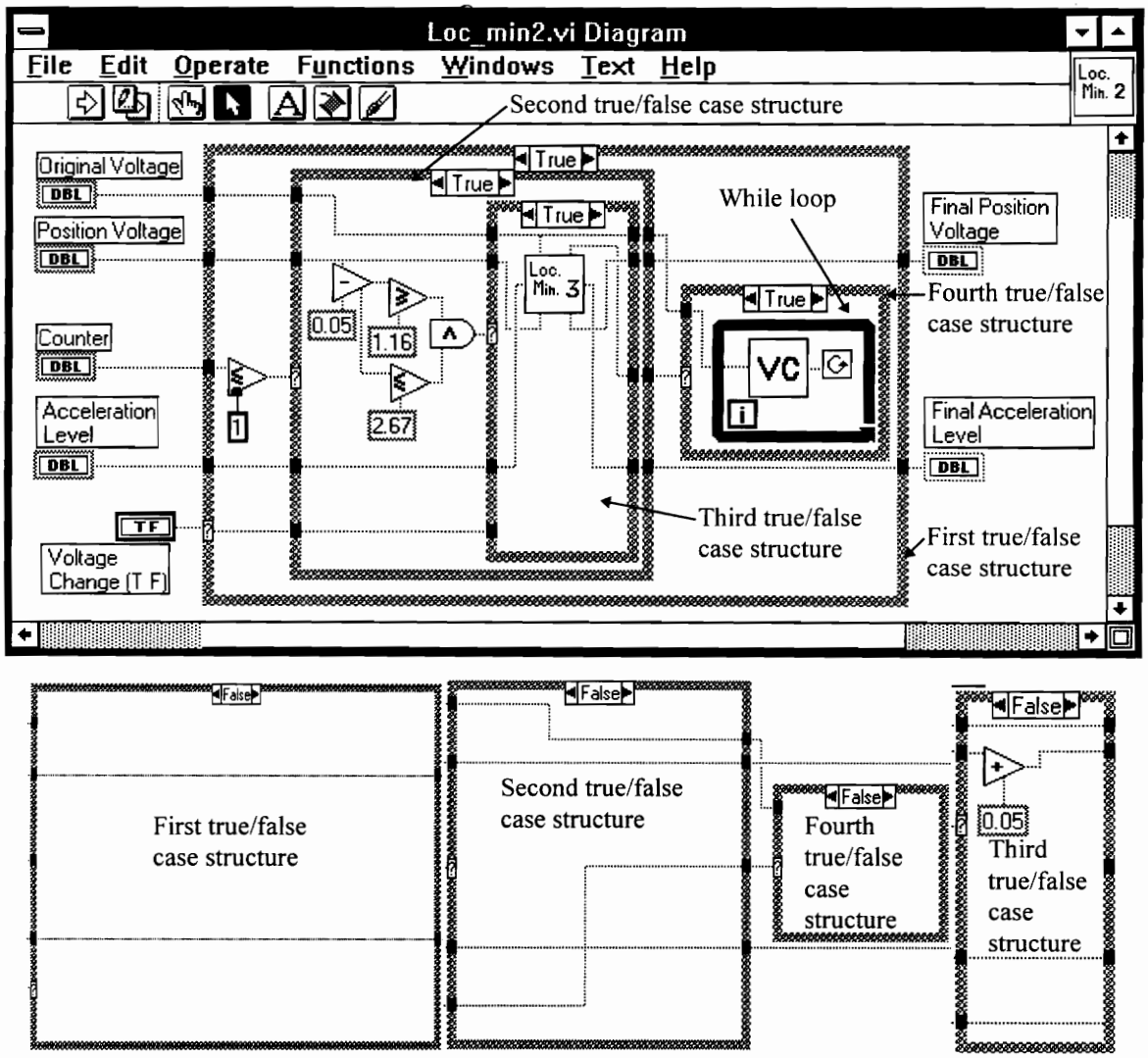

Figure 4.14: Locate Minimum 2 VI for Locate Minimum VI

receives the original forcing frequency value, counter value, absorber motor position value, the true or false statement from the VC VI, and the most recent rms acceleration value from the Loc_min VI. The true or false statement from the voltage change true/false

indicator will determine if the true or false case structure for the first true/false case structure will be implemented. If the voltage change indicator has a true statement, the true case structure will be implemented; otherwise, the false case structure will be implemented.

The true case structure for the first true/false case structure begins by evaluating the counter value and then implementing the internal second true/false case structure. If the counter value is less than or equal to one, a true statement is sent to the second true/false case structure; otherwise, a false statement is sent to the second true/false case structure. The first true/false case structure's false case structure bypasses the second, third, and fourth true/false case structures by passing the absorber motor position value to the final absorber motor position value indicator and/or calling program and passing the rms acceleration value to the final rms acceleration value indicator and/or calling program.

The true case structure for the second true/false case structure decreases the absorber motor position value by 0.05 units and verifies if this new value is greater than or equal to 1.16 and less than or equal to 2.67. If the new absorber motor position value is within this range, a true statement is sent to the third true/false case structure; otherwise, a false statement is sent to the third true/false case structure. The false case structure for the second true/false case structure bypasses the third true/false case structure by passing the original forcing frequency value and the true statement from the voltage change indicator to the fourth true/false case structure. The false case structure for the second true/false case structure also passes the absorber motor position value and the rms acceleration level to the end of the first true/false case structure.

The true case structure for the third true/false case structure implements the Loc_min3 VI. The Loc_min3 VI will be discussed later in this chapter. The false case for the third true/false case structure decreases the absorber motor position value by 0.05 units and

passes this new absorber motor position value along with the original forcing frequency value, rms acceleration level, and the true statement from the voltage change indicator to the end of the second true/false case structure.

The true case for the fourth true/false case structure implements a while loop. The while loop uses the original forcing frequency value to implement the VC VI discussed earlier in the chapter. As long as the VC VI returns a true statement the while loop will continue to operate. The false case for the fourth true/false case structure has no operations; therefore, the fourth case structure ceases execution.

4.2.2.6 Locate Minimum Three (Loc_min3) VI

Figure (4.15) shows the Loc_min3 VI. The Loc_min3 VI is a sub VI of Loc_min2 VI. Both VI's are part of the gradient search routine of the main program. The Loc_min3 VI receives the original forcing frequency value, absorber motor position value, and the most recent rms acceleration value from the Loc_min2 VI. These values are sent to the right side shift register of a while loop. The while loop continues to run as long as the forcing frequency value does not change or the absorber motor position value remains within the specified bandwidth. The first operation for the while loop is to implement the VC VI. The VC VI checks if the forcing frequency value has changed. The true or false statement from the VC VI will determine if the true or false case structure of the first true/false case structure will be implemented. If the statement from the VC VI is true, the true case structure will be implemented; otherwise, the false case structure will be implemented.

The true case structure for the first true/false case structure verifies if the absorber motor position value is greater than or equal to 1.16 and less than or equal to 2.67. If the new absorber motor position value is within this range, a true statement is sent to the second true/false case structure; otherwise, a false statement is sent to the second true/false case structure. The false case structure for the first true/false case structure bypasses the

second and third true/false case structures by passing the rms acceleration level and absorber motor position value to the end of the first true/false case structure. The false

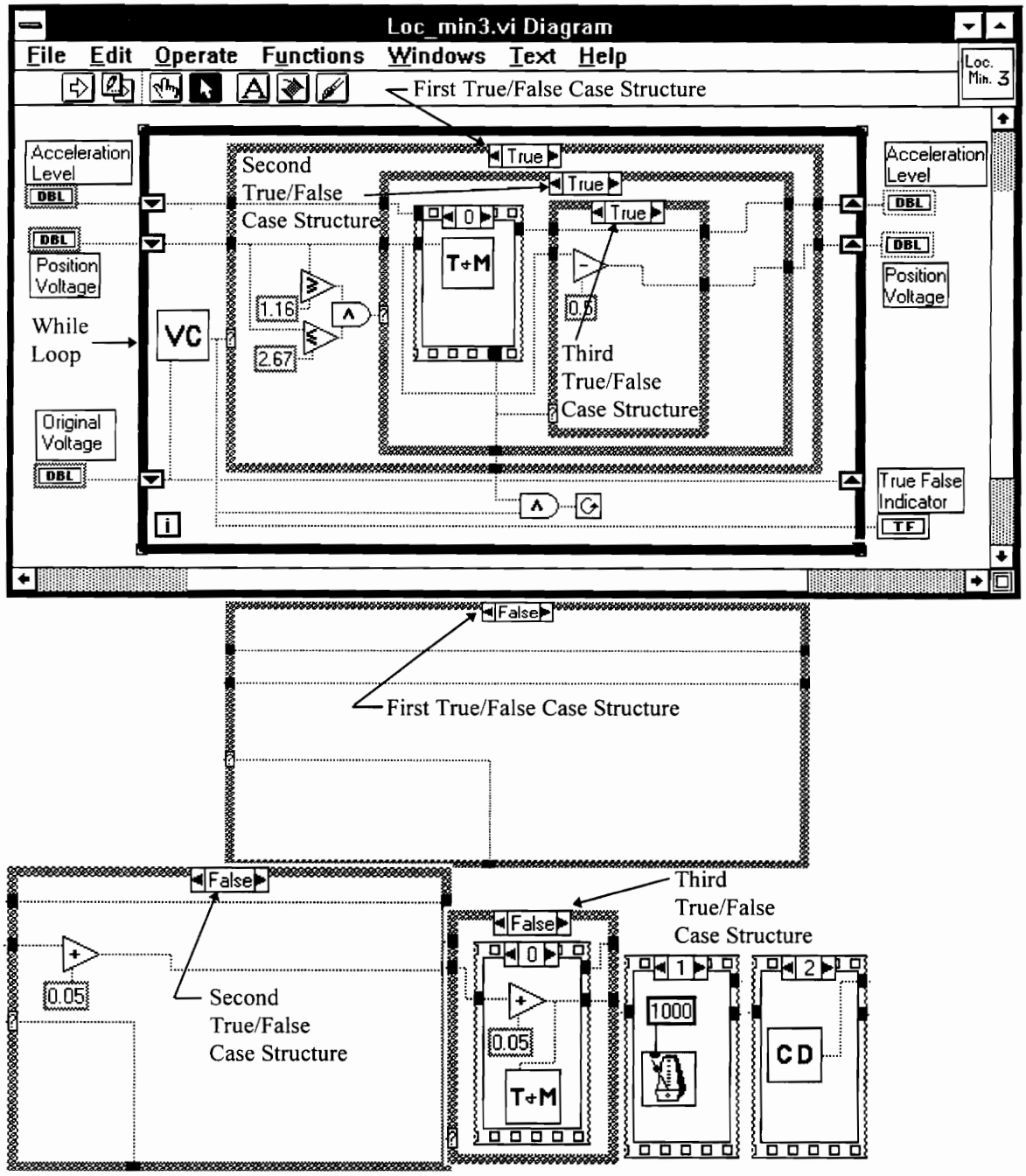

Figure 4.15: Locate Minimum 3 VI for Locate Minimum 2 VI

case structure for the first true/false case structure also passes the false statement from the VC VI to the end of the first true/false case structure. This false statement is passed to the operator for the while loop.

The true case structure for the second true/false case structure begins by implementing a sequence structure. The sequence structure consists of three frames that transfer the absorber motor to its new position, collect new rms acceleration levels, and compare the rms acceleration levels of the new absorber motor position with the previous absorber motor position. If the rms acceleration values of the new absorber motor position decrease then a true statement is sent to the third true/false case structure and the operator for the while loop. If the rms acceleration values of the new absorber motor position increase, a false statement is sent to the third true/false case structure and the operator for the while loop. The false case structure for the second true/false case structure increases the absorber motor position value by 0.05 units. The new absorber motor position voltage value and the rms acceleration level are sent to the end of the second true/false case structure. The false statement from the bandwidth check is also sent to the end of the second true/false case structure. This false statement is passed to the operator for the while loop.

The true case for the third true/false case structure decreases the absorber motor position value by 0.05 units. The new absorber motor position value and rms acceleration value are sent to the end of the third true/false case structure. The false case structure for the third true/false case structure implements a three frame sequence structure to reduce the absorber motor position value by 0.05 units, move the absorber motor to the new absorber motor position, and collect the rms acceleration level at the new absorber motor position. The new absorber motor position value and new rms acceleration value are sent to the end of the third true/false case structure.

4.3 Summary

In this chapter we have presented the control program LabView. We first presented a description of the initialization process for the absorber structure on the combined system. We covered the main program for controlling the absorber structure on the combined system. In the main program we presented the table look-up portion of the control program and the gradient search portion of the control program

For the next chapter, Chapter 5, we will present the hardware set-up and procedures for the experiments performed for the evaluation of the adaptive absorber system.

Chapter 5

5. Experiments

In this chapter we explain the hardware set-up and procedures for the experiments performed for the evaluation of the adaptive absorber system. The experiments are divided into three sections: preliminary experiments, initialization, and adaptive vibration absorber evaluation.

5.1 Preliminary Experiments

Before we could perform the final experiments or initialize the system, preliminary experiments had to be completed to determine settings of the instrumentation and values used in the control program. This section will cover those tests necessary before initializing the system and completing the final experiments.

5.1.1 Primary Structure Natural Frequency

The first piece of information needed was the frequency of the primary structure. The primary structure consists of the primary beam and attachment hardware for the absorber structure. A shaker test was completed to determine the primary structure's first bending natural frequency.

5.1.1.1 Set-up

Figure (5.1) is a schematic of the set-up for this experiment. A shaker is coupled to a force transducer via a stinger. The force transducer is screwed on to the primary beam. The shaker voltage input is connected to the voltage output of the Fourier analyzer through an amplifier. A voltmeter is used to read the voltage output of the amplifier. The shaker specifications require that the shaker input voltage never exceed 3.5 Volts. The accelerometer, placed on the primary beam and with a sensitivity of 96.6 mV/g, is

connected to channel two of the Fourier analyzer through a piezotron coupler. The force transducer, placed on the primary beam and with a sensitivity of 20.7 mV/N, is connected to channel one of the analyzer through a piezotron coupler. The analyzer is connected to a PC computer and communicates to the PC computer via the Tektronix 2600 series application library.

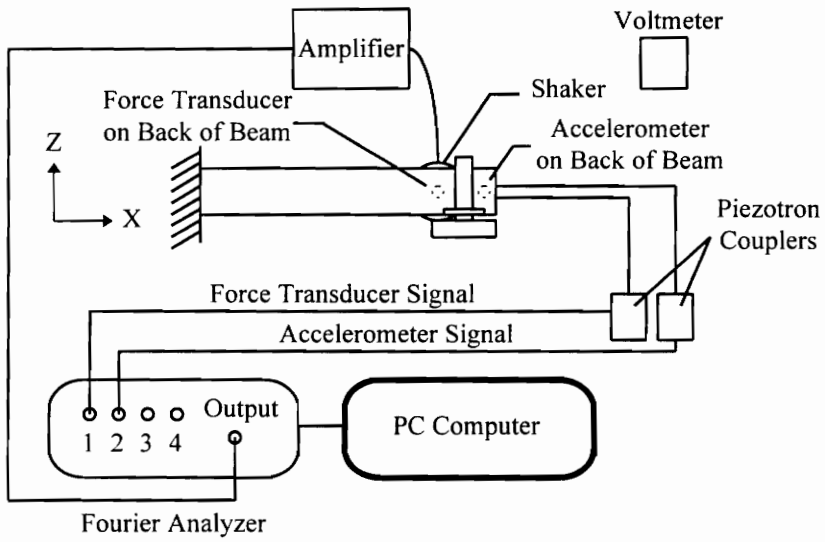

Figure 5.1 Experimental Set-up for Primary Structure Evaluation

5.1.1.2 Procedure

At a distance of 26.0 cm along the axis of the primary beam with respect to the edge of the clamp, the base and clearance beam were centrally attached (see Fig. (5.2)). The primary structure consists of the primary beam and attachment hardware for the absorber structure.

The transfer function graph (output-accelerometer/input-force transducer) and phase plots were used to detect the first bending natural frequency of the primary structure. A random input, a base band input from zero to 200 Hz, was used to drive the shaker. A total of 10 frequency response functions were produced and averaged. In addition, Hanning

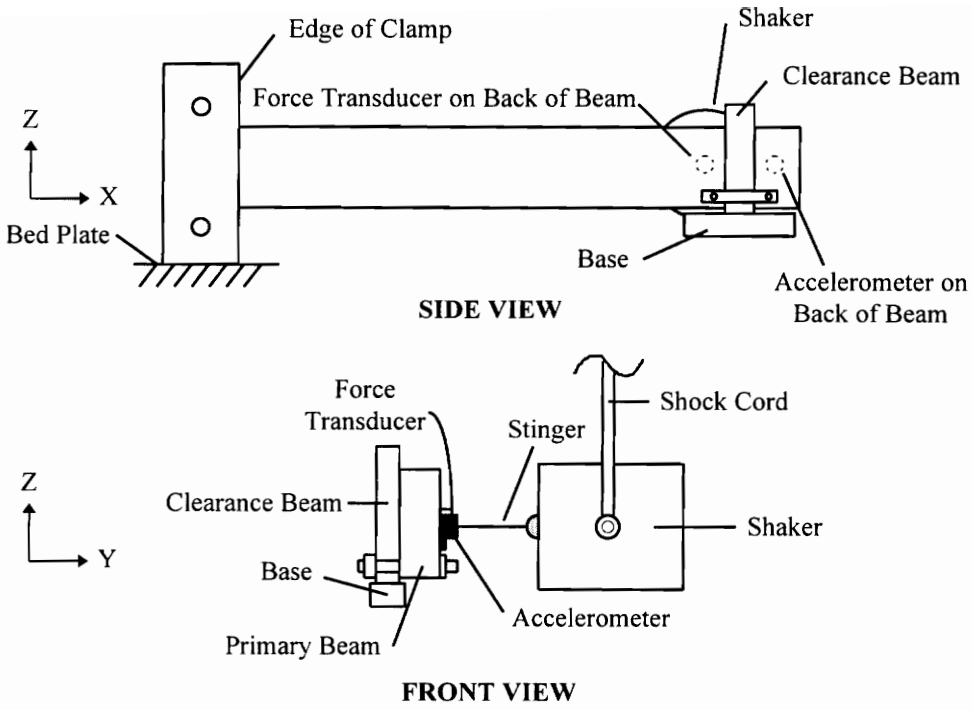

Figure 5.2: Physical Set-up for Primary Structure Evaluation

windowing with amplitude window correction was applied to the force and acceleration data so that noise could be eliminated. The input from the accelerometer and force transducer were autoranged to obtain the full dynamic range of the accelerometer and force transducer. Overload reject was used so that if at any time the accelerometer or force transducer overloaded, the corresponding block of data was not recorded. The coherence graph was used to verify the quality of data.

5.1.2 Adaptive Absorber Frequency Range

It was also important to verify that the absorber frequency range included the primary structure's natural frequency. Therefore, the absorber frequency range was evaluated. For these preliminary tests, the absorber was applied to the primary structure. Shaker tests were completed to determine the absorber frequency range.

5.1.2.1 Set-up

Figure (5.3) is a schematic of the set-up for this experiment. A shaker is coupled to a force transducer via a stinger. The force transducer is screwed on to the primary beam.

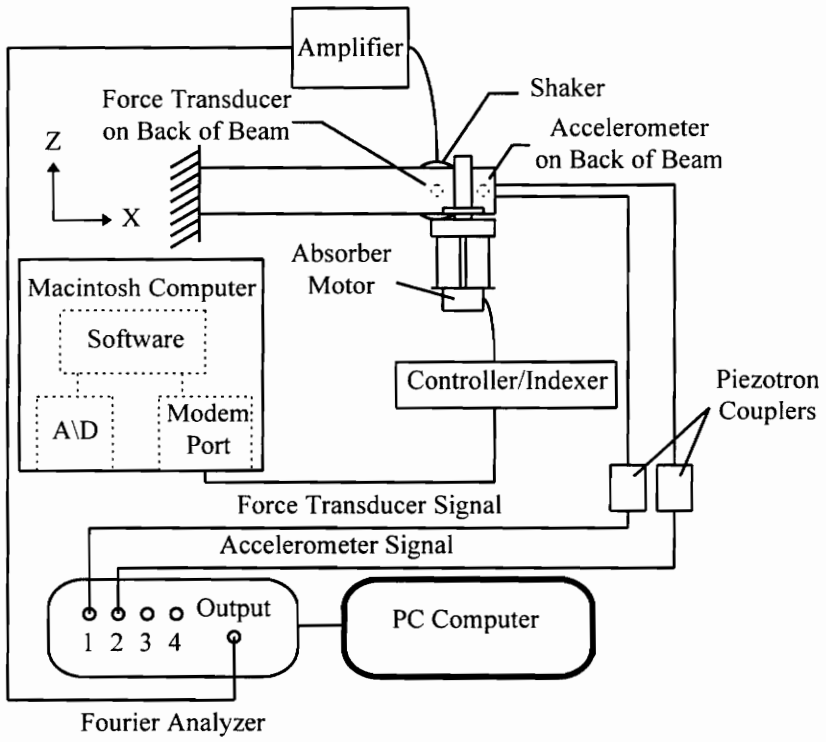

Figure 5.3: Experimental Set-up for Absorber Frequency Range Evaluation

The shaker voltage input is connected to the voltage output of the Fourier analyzer through an amplifier. A voltmeter is used to read the voltage output of the amplifier. The shaker specifications require that the shaker input voltage never exceed 3.5 Volts. The accelerometer, placed on the primary beam and with a sensitivity of 96.6 mV/g, is connected to channel two of the Fourier analyzer through a piezotron coupler. The force transducer, placed on the primary beam and with a sensitivity of 20.7 mV/N, is connected to channel one of the analyzer through a piezotron coupler. The analyzer is connected to a PC computer and communicates to the PC computer via the Tektronix 2600 series application library. The absorber motor is connected to the controller/indexer. The

controller/indexer is connected to the Macintosh computer and communicates with LabView via the modem port.

5.1.2.2 Procedure

At a distance of 26.0 cm along the axis of the primary beam with respect to the edge of the clamp, the absorber was attached to the base (see Fig. (5.4)). The absorber structure consists of the stepper motor, threaded rod, coupler, and guiding rods.

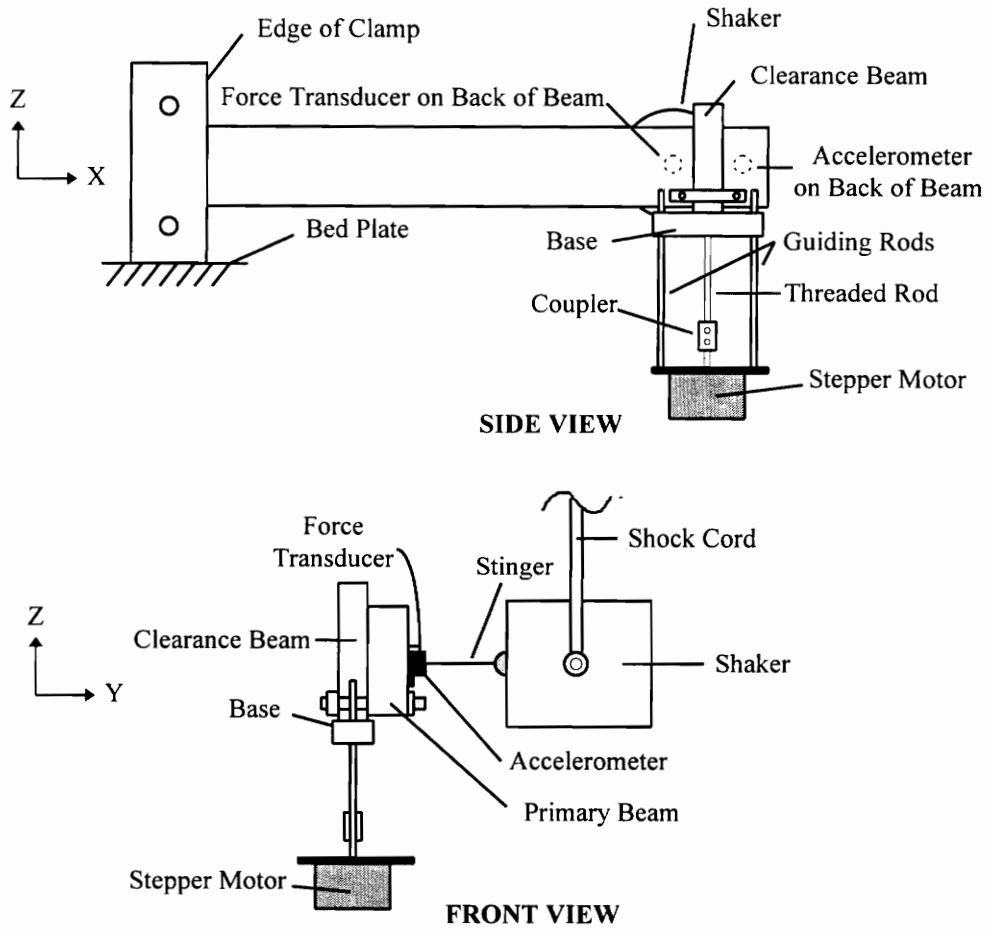

Figure 5.4: Physical Set-up for Absorber Frequency Range Evaluation

The transfer function graph (output-accelerometer/input-force transducer) and phase plots were used to detect the anti-resonant frequency of the combined system for the highest and lowest setting of the absorber motor. The range of the absorber had to include the

natural frequency of the primary structure and this result was verified. Also, frequency response functions were taken for intermediate locations of the absorber motor to determine the relationship between the absorber position and the anti-resonance of the combined system. A random input, a base band input from zero to 200 Hz, was used to drive the shaker. A total of 10 frequency response functions were produced and averaged. In addition, Hanning windowing with amplitude window correction was applied to the force and acceleration data so that noise could be eliminated. The input from the accelerometer and force transducer were autoranged to obtain the full dynamic range of the accelerometer and force transducer. Overload reject was used so that if at any time the accelerometer or force transducer overloaded, the block of data was not recorded. The coherence graph was used to verify the quality of data.

5.1.3 Absorber Motor Home Position

The next experiment involved finding a measurable relationship to a home position of the absorber motor. The home position was selected to be when the absorber is at its highest frequency setting. This worked best with the Philtec displacement sensor used when it was mounted to the base.

5.1.3.1 Set-up

Figure (5.5) is a schematic of the set-up for determining the voltage output from the Philtec displacement sensor when the absorber motor is at the home position. The displacement sensor is mounted through a vertical hole located on the base at a distance of 28.86 cm from the edge of the clamp. Since the displacement sensor is an optic sensor that works best with a mirror like surface, a piece of aluminum foil was placed on the absorber motor to increase the reflectivity of the absorber motor flange surface. A power supply is connected to the displacement sensor through its input terminals. A voltmeter is also connected to the displacement sensor through its output terminals.

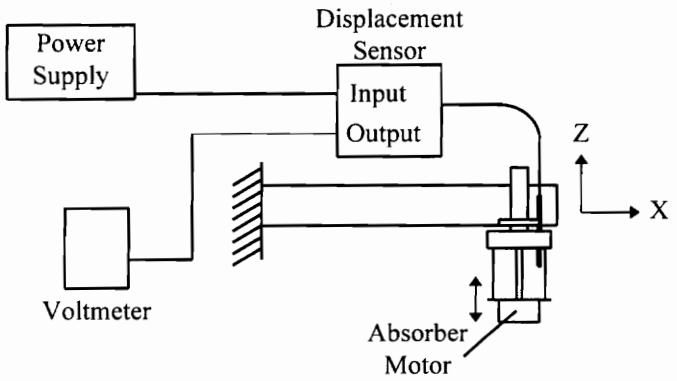

Figure 5.5: Experimental Set-up for Determining Absorber Home Position

5.1.3.2 Procedure

A voltage reading was obtained when the absorber motor was at its highest frequency setting. The voltage value outputted by the sensor for the absorber in this position is used as the control for the initialization process and for setting the home position of the absorber in future tests.

5.1.4 Relationship Between Input Voltage and Forcing Frequency

Another test was necessary to determine the settings of the function generator. It is necessary due to limitations of the A/D board and function generator that the voltage range of 0-5 volts results in a frequency range that encompasses both shift points of the absorber. This information was also necessary in determining the relationship between the Voltage source voltage and the absorber motor position and the relationship between the Voltage source voltage and the forcing frequency.

5.1.4.1 Set-up

Figure (5.6) is a schematic of the set-up for determining the function generator settings. A voltage source is connected to the VCG function generator at its VCG in terminal. A voltmeter is also connected to the voltage source. An oscilloscope is connected to the signal output of the function generator.

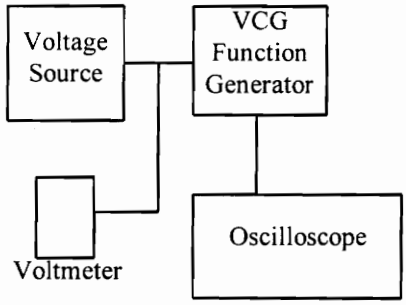

Figure 5.6: Experimental Set-up for Determining the Function Generator Settings

5.1.4.2 Procedure

The voltmeter was used to obtain a more precise voltage reading from the voltage source. From the previous experiments, a frequency range corresponding to the voltage range of 0-5 Volts was known. The oscilloscope was used to verify that the sine output from the function generator for the voltage range indeed spans the necessary frequency range.

5.2 Initialization

As a preliminary step between turning on all the equipment and performing the final experiments, the controller/indexer had to be initialized and the absorber motor set to its home position. This section will cover the initialization and homing process.

5.2.1 Set-up

Figure (5.7) is a schematic of the set-up for initializing the controller/indexer and setting the absorber motor home position. The displacement sensor is mounted through a vertical hole located on the base at a distance of 28.86 cm from the edge of the clamp. Since the displacement sensor is an optic sensor that works best with a mirror like surface, a piece of aluminum foil was placed on the absorber motor to increase the reflectivity of the absorber motor flange surface. A power supply is connected to the displacement sensor through its input terminals. The output terminal of the displacement sensor is connected to the Macintosh computer software via the A/D board. The computer software is also

connected to the controller/indexer via the modem port. The controller indexer is connected to the stepper motor. The computer software, LabView, was used for the initialization and setting of home position process.

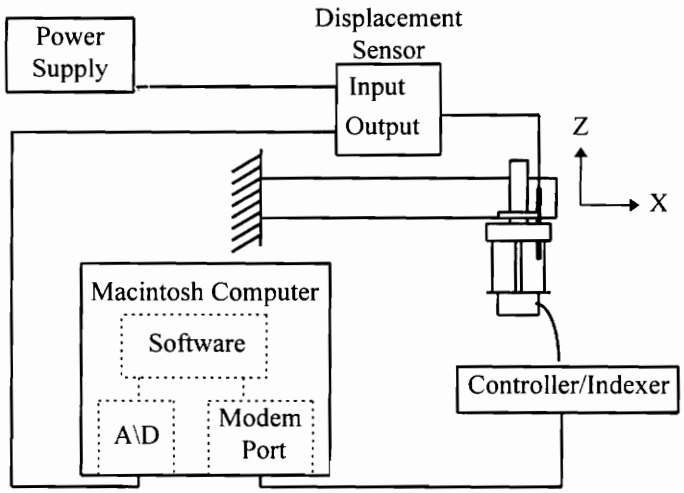

Figure 5.7: Experimental Set-up for Initialization Process and Setting Home Position

5.2.2 Procedure

The first process was the initialization of the controller/indexer. Once the controller/indexer was initialized, it would be ready to receive commands from LabView through the modem port. Initializing the controller/indexer requires a space followed by a carriage return. Next, the LabView initialization program would monitor the voltage output from the Philtec displacement sensor through the A/D board. If the voltage from the displacement sensor is smaller than the voltage value predetermined from the earlier, absorber home position, experiment when the motor is in the home position, then LabView would send a command to the controller/indexer for the motor to step a predetermined step size toward the sensor. Due to the large step size the motor position tends to overshoot causing the final voltage readout from the displacement sensor to be larger than the control voltage. Once the displacement sensor voltage is larger than the control voltage, LabView sends a command to the controller/indexer instructing the motor to step a smaller predetermined step size away from the sensor. Again, due to the

step size the motor position tends to overshoot causing the final voltage readout from the displacement sensor to be smaller than the control voltage. Once the displacement sensor voltage is smaller than the control voltage, LabView sends a command to the controller/indexer instructing the motor to step at its smallest step size toward the sensor until the sensor voltage equals the control voltage value. The motor is now located in the home position. After this process, LabView sends commands to the controller/indexer to set this position of the motor as the home position or zero position. After the completion of the initialization process, the experimental set-up is ready to perform the final experiments.

5.3 Adaptive Vibration Absorber Evaluation

After the completion of the preliminary tests, initialization of the controller/indexer, and setting the absorber motor home position, we are ready to perform the final experiments. This section will cover the experimental set-up for completing the final experiments and the procedure for collecting the final experiments data.

5.3.1 Set-up

Figure (5.8) is a schematic of the set-up for this experiment. A shaker is coupled to a force transducer via a stinger. The force transducer is screwed on to the primary beam. The shaker is connected to the output of the function generator through an amplifier. A voltage source is connected to the VCG in of the function generator. A voltmeter is used to read off the voltage source in order to obtain an accurate reading of the voltage output. The DC voltage is also read by LabView via the A/D board of the Macintosh computer. The accelerometer, placed on the primary beam and with a sensitivity of 96.6 mV/g, is connected to channel two of the Fourier analyzer through a piezotron coupler. The force

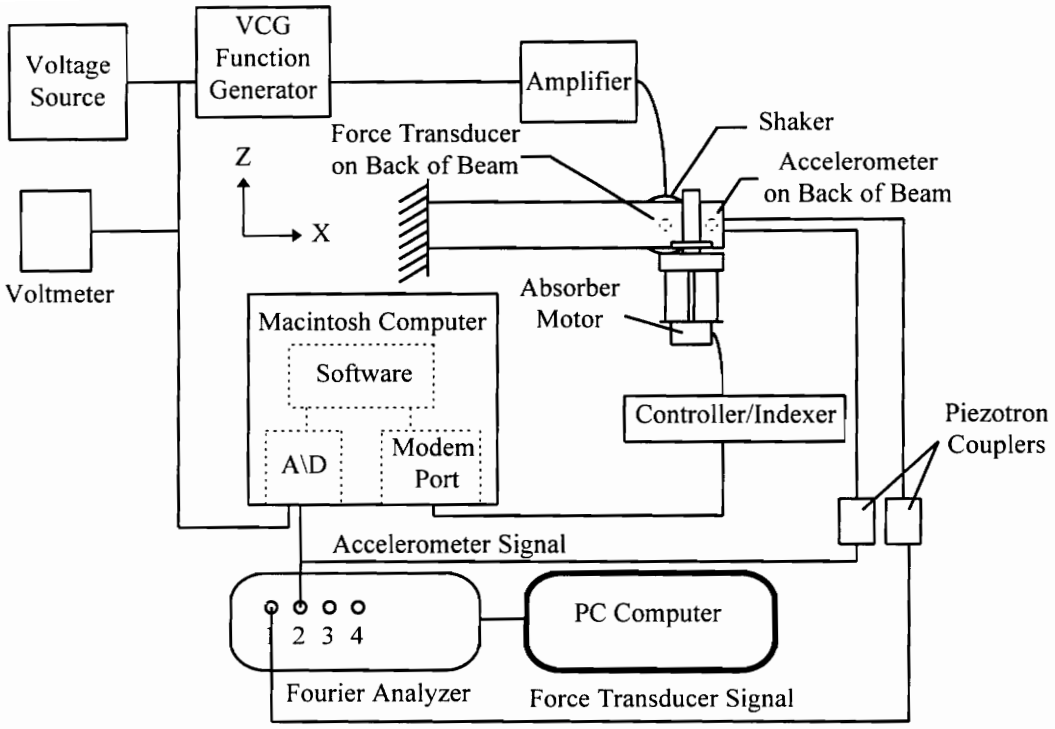

Figure 5.8: Experimental Set-up for Adaptive Vibration Absorber Evaluation

transducer, with a sensitivity of 20.7 mV/N, is connected to channel one of the analyzer through a piezotron coupler. The analyzer is connected to a PC computer and communicates to the PC computer via the Tektronix 2600 series application library. The accelerometer signal is also read by LabView via the A/D board of the Macintosh computer. LabView is connected to the controller/indexer via the modem port of the Macintosh computer. The absorber motor is connected to the controller/indexer.

5.3.2 Procedure

At a distance of 26.0 cm along the axis of the primary beam with respect to the edge of the clamp, the absorber is attached to the base (see Fig. (5.9)). The absorber structure consists of the stepper motor, threaded rod, coupler, and guiding rods.

The source voltage is incremented by 0.2 Volts from 0 Volts to 5.0 Volts and data is collected at each value. Each 0.2 Volt increment results in a 4.0 Hz increment of the

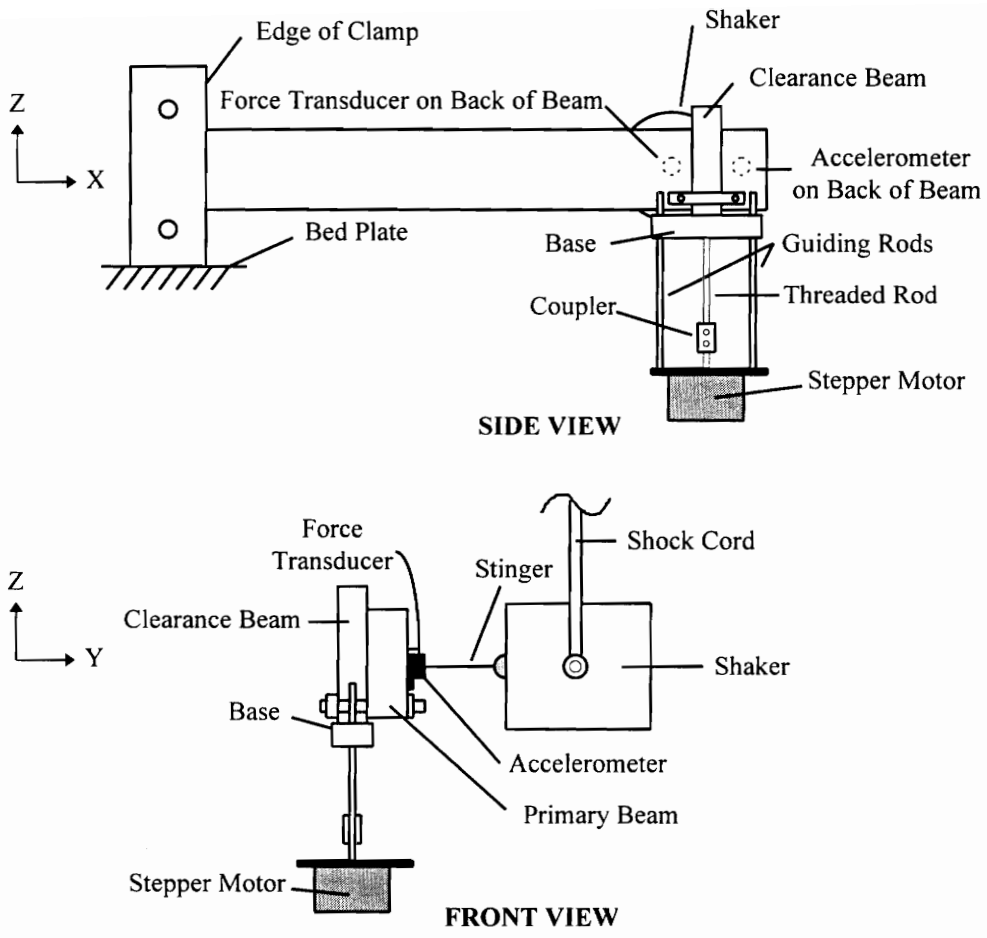

Figure 5.9: Physical Set-up for Adaptive Vibration Absorber Evaluation

function generator for a total frequency range of 30.0 Hz to 130.0 Hz. Data is also taken at non-incremental frequencies around critical frequency points such as the shift frequency points of the adaptive absorber and near the primary structure natural frequency. Shift frequency points are defined as where the absorber transitions from its highest frequency location to its lowest frequency location and vice-versa. The autospectrum graph of both the accelerometer and the force transducer are used to calculate the magnitude of the frequency response function at the forcing frequency. The phase plot is also evaluated to determine the phase at the current forcing frequency. A sine input is used to drive the shaker. The frequency of the excitation force is determined by the Voltage source voltage. A total of 10 time averages are taken for each frequency. In addition, Hanning windowing with amplitude window correction is applied to the force

and acceleration data so that noise could be eliminated. The input from the accelerometer and force transducer are autoranged to obtain the full dynamic range of the accelerometer and force transducer. Overload reject is used so that if at any time the accelerometer or force transducer overloads, the block of data is not recorded. The coherence graph is used to verify the quality of data.

5.4 Summary

In this chapter, we have covered the hardware set-up and procedures for evaluation of the adaptive absorber system. The experiments were divided into three section: preliminary experiments, initialization, and final experiments. The experiment set-ups and procedures were described for each section.

For the next chapter, Chapter 6, we will present the results from our experiments, as presented in this chapter.

Chapter 6

6. Results

In this chapter we present the results obtained from our experiments performed in Chapter 5. This chapter is divided into three parts. First, we present the results from the preliminary experiments. Next, we present the results from the adaptive vibration absorber evaluation. Lastly, we will present comparisons for the different systems.

6.1 Result of the Preliminary Experiments

This section will cover the results of the preliminary experiments. These results are needed for the control program and for comparisons in the final evaluations.

6.1.1 Primary Structure Natural Frequency

Using the testing procedure described in Chapter 5 for the primary structure, the primary structure's frequency response function is obtained. Figure (6.1) is the graph of the frequency response function of the primary structure obtained from the experimental data showing the resonance corresponding to the 1^{st} structure mode. The transfer function magnitude plot and phase plot are used to determine the natural frequency of the primary structure. Results from this data yield a 1^{st} mode natural frequency of 72 Hz.

Next, the absorber frequency range is evaluated to confirm that the primary structure natural frequency is within the absorber frequency range. The next section will present the results obtained for the absorber frequency range experiments.

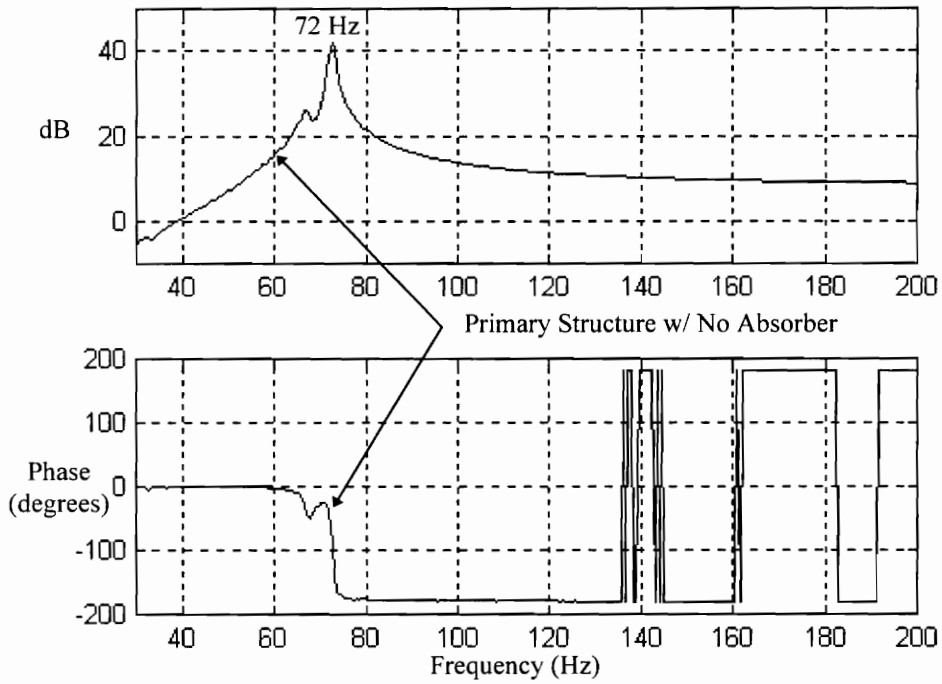

Figure 6.1: FRF of the 1st Mode of the Primary Structure

6.1.2 Adaptive Absorber Frequency Range

Using the testing procedure described in Chapter 5 for the absorber frequency range, the combined system's frequency response functions are obtained. Figure (6.2) is the frequency response function graph of the combined system for the absorber's longest length of 8.89 cm, measured from bottom edge of base to top of motor flange. The transfer function magnitude plot and phase plot are used to determine the anti-resonant frequency of the combined system. Recall from Chapter 2 that the natural frequency of the absorber structure corresponds to the anti-resonance of the combined system. Results from this data yield the absorber's lowest natural frequency to be 53.5 Hz.

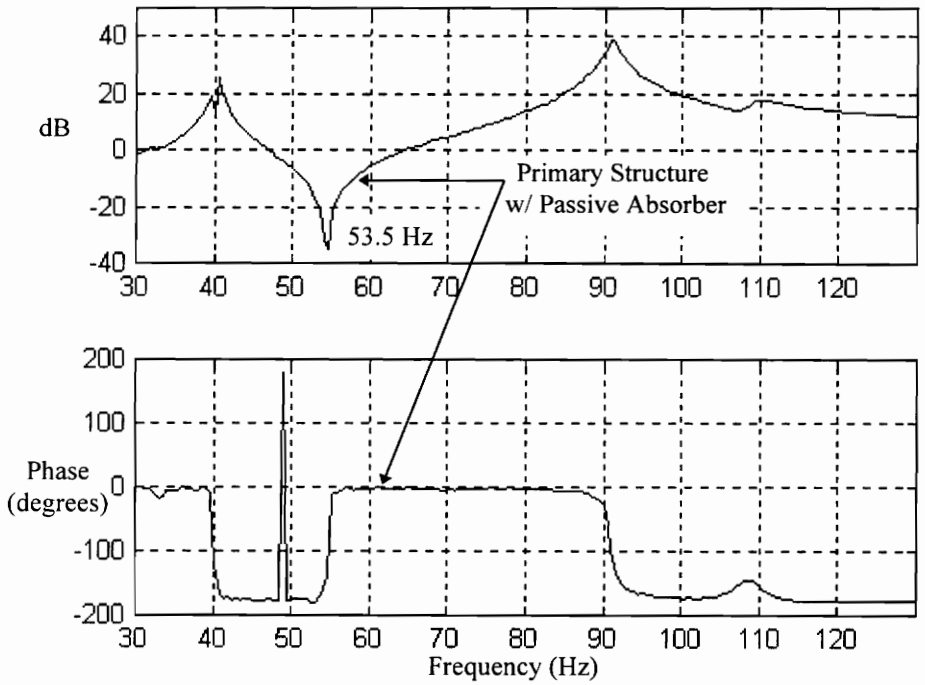

Figure 6.2: FRF of the System with the Absorber Tuned at Lowest Frequency

Figure (6.3) is the frequency response function graph of the combined system for the absorber's shortest length of 5.08 cm. Results from this data yield the absorber's highest natural frequency to be 84.0 Hz.

Table (6.1) shows the system anti-resonant frequencies (absorber natural frequencies) versus incremental absorber lengths. This table shows that for an absorber length range of 5.08 cm to 8.89 cm the absorber natural frequency ranges from 84.0 Hz to 53.5 Hz, respectively. This corresponds to a 1.0 cm per 8.0 Hz length to frequency ratio. Also, these results are summarized in Fig. (6.4). Figure (6.4) shows the linear relationship between absorber length and absorber frequency for this absorber's range of frequencies. This information is needed in the control program for leading to a relationship between the input voltage and the absorber motor position.

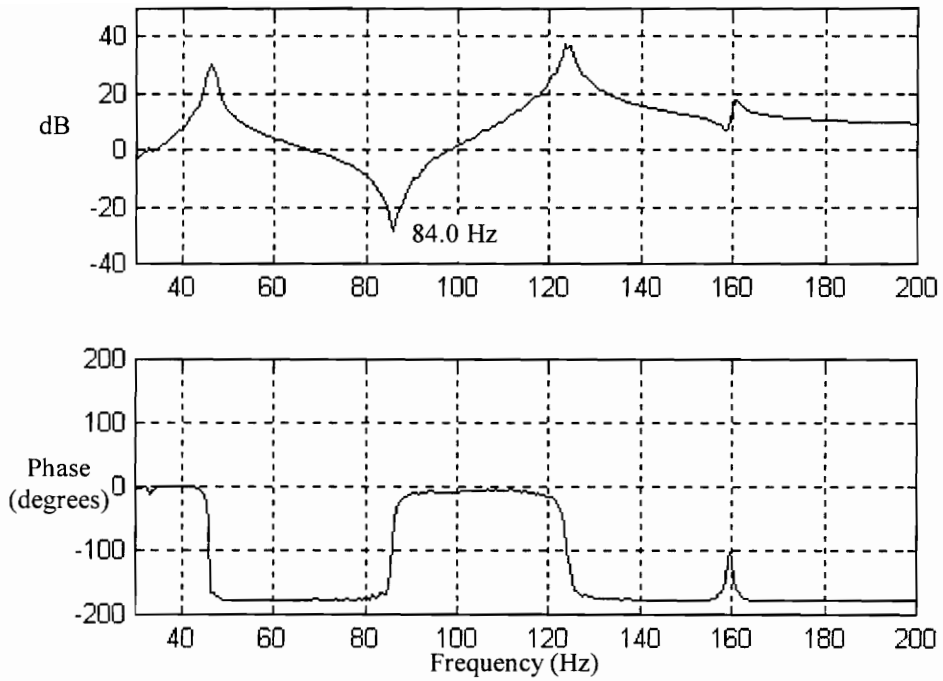

Figure 6.3: FRF of the System with the Absorber Tuned at Highest Frequency

Table 6. 1: System Anti-Resonant Frequency vs. Absorber Length

Base to Flange Length (cm)	Anti-Resonant Frequency (Hz)
5.08	84.0
5.72	78.5
6.35	72.0
6.99	66.0
7.62	62.5
8.26	57.5
8.89	53.5

Next, the absorber motor home position had to be determined such that a relationship between the absorber control position and the absorber natural frequency could be

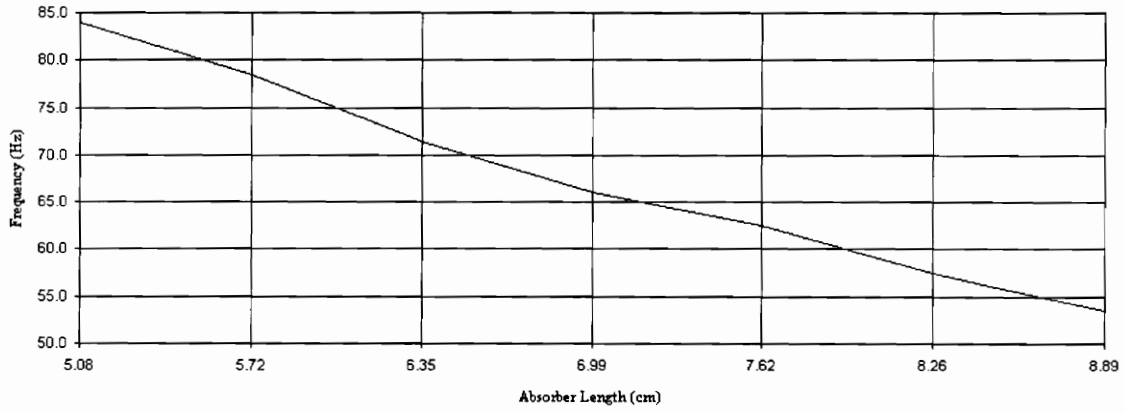

Figure 6.4: System Anti-Resonance Frequency vs. Absorber Length

determined. The next section will present the results obtained for determining the relationship between absorber control position and the absorber natural frequency.

6.1.3 Absorber Motor Home Position

Using the testing procedure described in Chapter 5 for determining the absorber motor home position, the displacement sensor voltage is found to be 1.14 Volts. This voltage corresponded to a home position of zero, an absorber length of 5.08 cm, and an absorber frequency of 84.0 Hz. A clockwise rotation of the absorber motor shaft (looking from primary structure to motor) results in a negative step for the motor position. Since the threaded rod used is 20 turns per 2.54 cm and the absorber motor resolution is 200 steps per turn, a clockwise rotation of the absorber motor shaft to an absorber length of 8.98 cm results in a motor position of -6000 and an absorber frequency of 53.5 Hz. This motor position resolution information results in a relationship of 1539 steps per 1.0 cm of change in absorber length.

Next, the function generator settings are determined such that a relationship between DC power supply voltage and the forcing frequency could be determined. The next section

will present the results obtained for determining the relationship between input voltage and forcing frequency.

6.1.4 Relationship Between Input Voltage and Forcing Frequency

Using the testing procedure described in Chapter 5 for determining the relationship between input voltage and forcing frequency, the following relationships are obtained. Table (6.2) shows the function generator frequency versus DC power supply voltage. This table shows that for an input voltage range of 0.0 Volts to 5.0 Volts there is a forcing frequency of 29.85 Hz to 131.58 Hz, respectively. This corresponds to a 20.35 Hz change in forcing frequency per 1.0 Volt change in input voltage. Figure (6.5) graphically shows the linear relationship between the input voltage and the forcing frequency.

Table 6. 2: Function Generator Frequency vs. DC Power Supply Voltage

Volts	Frequency
0.0	29.85
0.5	40.00
1.0	50.25
1.5	60.60
2.0	71.43
2.5	80.64
3.0	90.90
3.5	101.01
4.0	111.73
4.5	121.95
5.0	131.58

A relationship of 3950 steps per 1.0 Volt input voltage is determined using: the previous relationships of 20.5 Hz change in forcing frequency per 1.0 Volt change in input voltage, a change of 1539 steps per 1.0 cm change in absorber length, a 1.0 cm change in absorber length per 8.0 Hz change in absorber natural frequency, and an absorber motor position

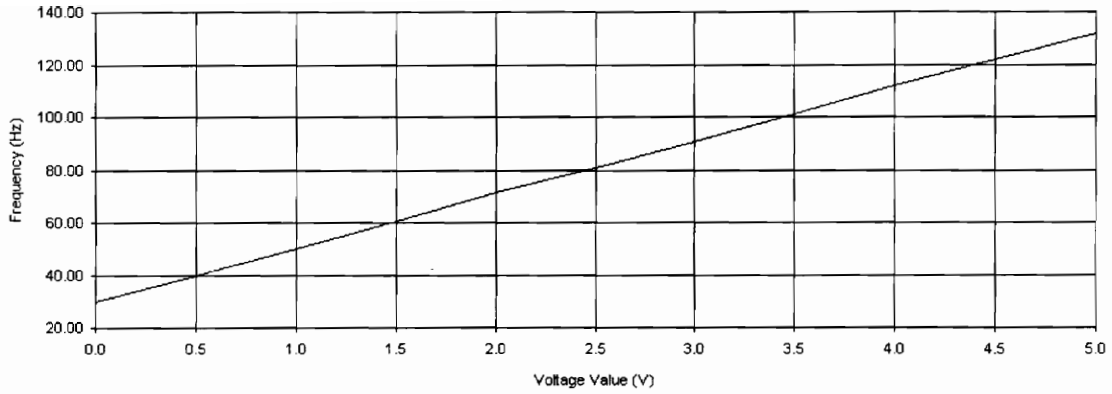

Figure 6.5: Function Generator Frequency vs. DC Power Supply Voltage

equal to the step number. Using an input voltage of 2.67 Volts and its relation to the zero motor position as well as the relationship between the motor position and the step value S, the following relationship is made between motor position P and input voltage V:

$$P = \frac{P}{S}(3950\frac{S}{V} * V - 10609 * S). \qquad 6.1$$

Once the preliminary experiments are completed and the controller/indexer initialized, the final control program can be executed and the final steady-state vibration amplitudes of the primary structure can be found for various steady-state forcing frequencies. The next section will present the final experiment's results for a primary structure with an adaptive absorber and comparisons of the primary structure with no absorber and the primary structure with a passive absorber.

6.2 Results of Final Experiments

Once the preliminary experiments are completed and the controller/indexer initialized, the final control program is executed and the final steady-state vibration amplitudes of the primary structure are found for various forcing frequencies. This section contains two

subsections. In the first section, we will present the steady-state vibration amplitude results for a primary structure with an adaptive absorber. In the last section, we will present comparisons of the primary structure with an adaptive absorber, the primary structure with no absorber, and the primary structure with a passive absorber

6.2.1 Adaptive Absorber Evaluation

In this section, we will present the vibration amplitude results for a primary structure with an adaptive absorber after the forcing frequency has reached a steady-state and the absorber has adapted to the forcing frequency. Figure (6.6) shows the frequency response function for the primary structure with an adaptive absorber. The frequency response function range of frequencies are from 30 Hz to 130 Hz. The transfer function magnitude

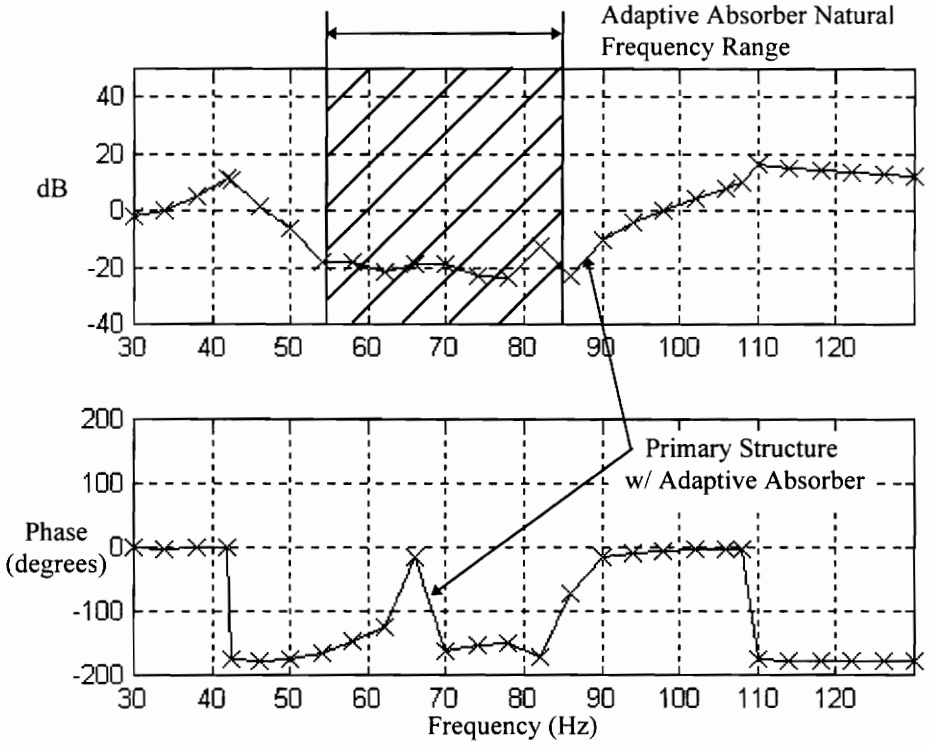

Figure 6.6: FRF of the System with the Adaptive Absorber

plot shows a maximum vibration amplitude of 16.4 dB at 110 Hz and a minimum of -23.5 dB at 78 Hz. Throughout the adaptive absorber tuning range of 54.0 Hz to 84.0 Hz the vibration amplitude is consistently around -20 dB. From the phase plot we expect to see a phase of 0 degrees for the ranges of 30 Hz to 42 Hz and 84 Hz to 108 Hz with a transition from 0 degrees to -180 degrees at 42 to 42.5 Hz and 108 Hz to 110 Hz. We expect the phase to be -180 degrees in the ranges of 42.5 Hz to 54.0 Hz and 110 Hz to 130 Hz. We expect the phase to be either 0 degrees or -180 degrees throughout the 54.0 Hz to 84.0 Hz. This varies, because, the optimization routine could easily settle at a frequency slightly lower (0 degrees) or slightly higher (-180 degrees) than the forcing frequency. The phase plot coincides with our assumptions of the phase. Throughout the adaptive absorber tuning range the absorber optimized at a frequency slightly lower than the forcing frequency. However, by evaluating the phase, at 66 Hz the absorber optimized at a frequency slightly higher than the forcing frequency.

By treating the absorber as a passive absorber tuned to the lowest and highest frequencies of the adaptive absorber tuning range, a transfer function is obtained at each frequency location. Figure (6.7) shows a comparison between the primary structure with an adaptive absorber versus the primary structure with a passive absorber tuned to the lowest frequency of the adaptive absorber tuning range. It is expected, from the control program, that the system with the adaptive absorber will have the same vibration amplitudes as the system with the passive absorber for the frequency ranges of 42.5 Hz to 54.0 Hz and 110 Hz to 130 Hz. This result is verified in this comparison. Figure (6.8) shows a comparison between the primary structure with an adaptive absorber versus the primary structure with a passive absorber tuned to the highest frequency of the adaptive absorber tuning range. It is expected, from the control program, that the system with the adaptive absorber will have the same vibration amplitudes as the system with the passive absorber for the frequency ranges of 30.0 Hz to 42.0 Hz and 84.0 Hz to 108 Hz. This result is verified in this comparison.

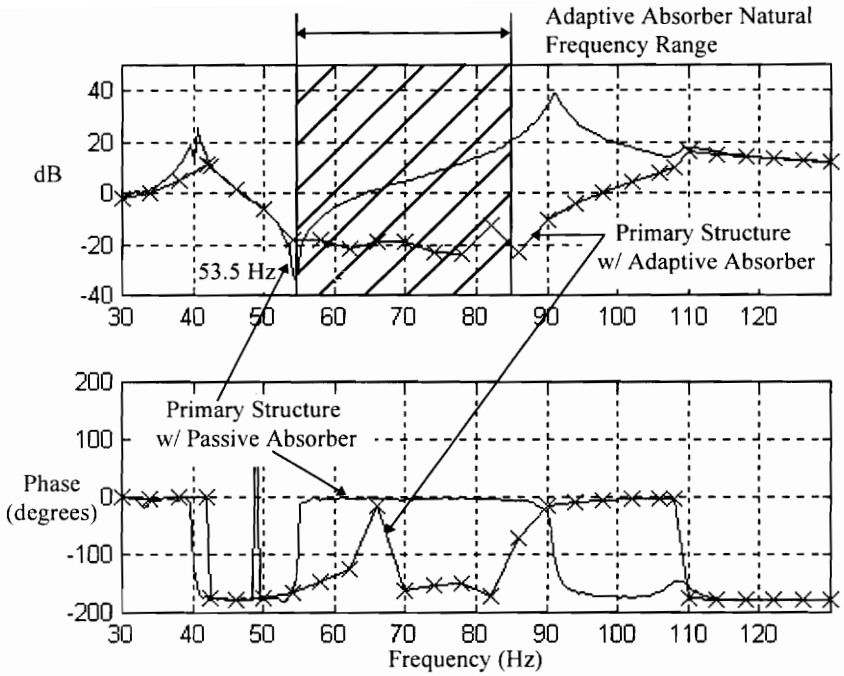

Figure 6.7: FRF of the System: Adaptive vs. Passive (Absorber length = 8.89 cm)

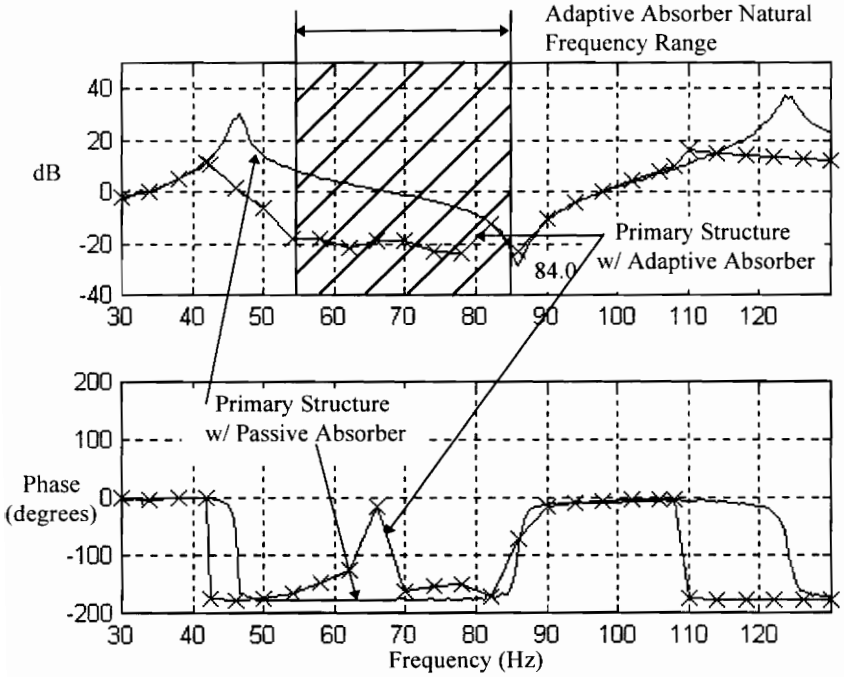

Figure 6.8: FRF of the System: Adaptive vs. Passive (Absorber length = 5.08 cm)

Next, we will present comparisons of the primary structure with an adaptive absorber, the primary structure with no absorber, and the primary structure with a passive absorber

6.3 Comparisons of Different Systems

In this section, we will present comparisons of the primary structure with an adaptive absorber, the primary structure with no absorber, and the primary structure with a passive absorber. First, we will present the frequency response function of the primary structure with a passive absorber (tuned to the natural frequency of the primary structure). Then, we will compare the primary structure with no absorber to the primary structure with the passive absorber. Next, we will present a comparison of the primary structure with no absorber to the primary structure with an adaptive absorber. Then, we will present a comparison of the primary structure with the passive to the primary structure with an adaptive absorber. Lastly, we will show a summarized comparison between the primary structure with no absorber, the primary structure with the passive absorber, and the primary structure with an adaptive absorber.

Figure (6.9) shows the transfer function magnitude plot and phase plot of the primary structure with a passive absorber (tuned to the natural frequency of the primary structure). From the transfer function magnitude plot and phase plot the resonant frequencies are located at 43.5 Hz and 108 Hz with amplitudes of vibration of 26 dB and 39 dB, respectively. The anti-resonant frequency is located at 72 Hz with a vibration amplitude of -30 dB. The glitch in the transfer function located at 144 Hz is twice the absorber natural frequency and can be attributed to impacts in the absorber structure.

Figure (6.10) shows a comparison of the transfer function magnitude plot and phase plot of the primary structure with no absorber to the primary structure with the passive

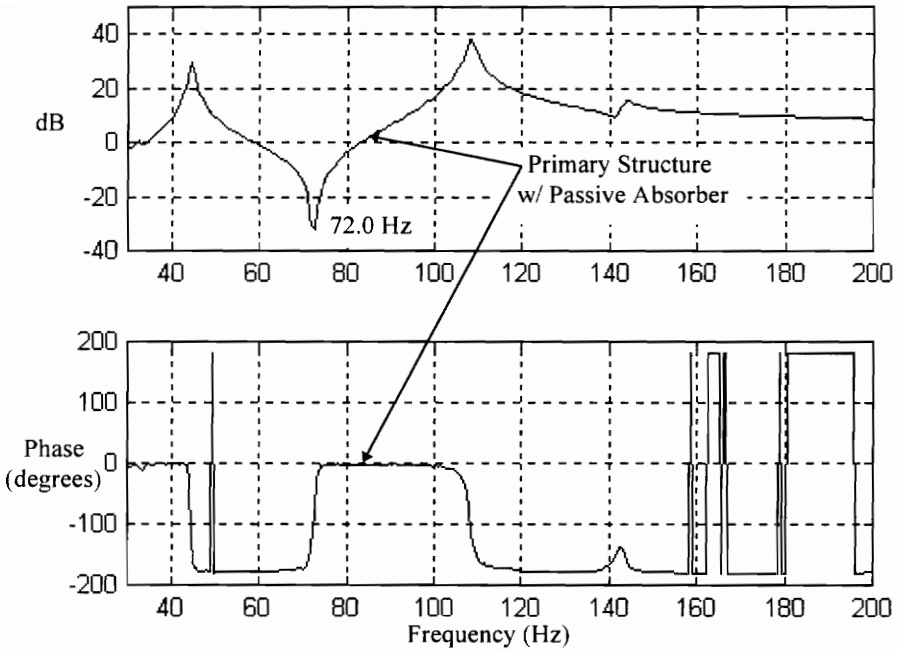

Figure 6.9: FRF of the System with Passive Absorber Tuned to Primary Structure's Natural Frequency

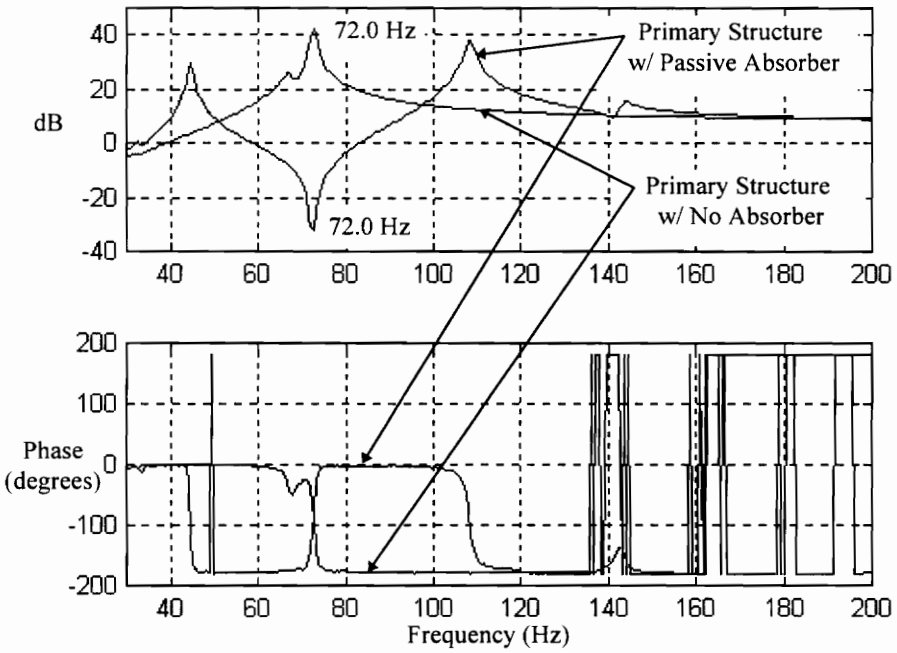

Figure 6.10: FRF of Primary Structure vs. Passive (Absorber length = 6.35 cm)

absorber (tuned to the natural frequency of the primary structure). As is expected, the system with the passive absorber offers significant reduction to the vibration amplitudes throughout the 50 Hz to 98 Hz range with reductions as much as 70 dB at the primary structure natural frequency. However, the tradeoff is that there now exists two resonances located at 43.5 Hz and 108 Hz. The system with the passive absorber increases the vibration amplitudes throughout the frequency ranges of 30 Hz to 50 Hz and 98 Hz to 180 Hz. Also, there are increases in vibration amplitudes as much as 27 dB at the second resonance of the passive absorber system.

Figure (6.11) shows a comparison of the transfer function magnitude plot and phase plot of a primary structure with no absorber to the primary structure with the adaptive absorber. As is expected, the system with the adaptive absorber offers significant reduction to the vibration amplitudes throughout the 45 Hz to 108 Hz range with reductions as much as 60 dB at the primary structure natural frequency. Also, the

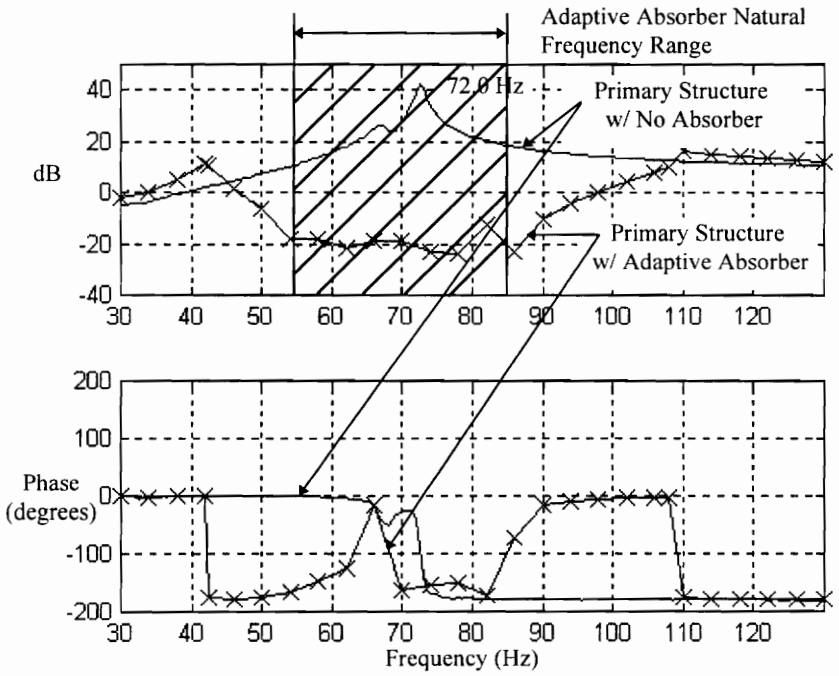

Figure 6.11: FRF of the Primary Structure vs. Adaptive Absorber

absorber consistently gives at least 30 dB reductions in vibration amplitude throughout the absorber tuning range of 54.0 Hz to 84 Hz. However, the tradeoffs are that there exists increases in vibration amplitudes throughout the frequency ranges of 30 Hz to 45 Hz and 108 Hz to 130 Hz with increases in vibration amplitudes as much as 10 dB at 42.5 Hz.

Figure (6.12) shows a comparison of the transfer function magnitude plot and phase plot of the primary structure with a passive absorber to the primary structure with an adaptive absorber. As is expected, the system with the adaptive absorber offers significant reduction to the vibration amplitudes throughout the 42 Hz to 71 Hz range and the 73 Hz to 130 Hz range with fairly consistent reductions of 20 dB throughout both ranges. However, the tradeoff is that there exists increases in vibration amplitudes throughout the frequency range of 71 Hz to 73 Hz with increases in vibration amplitudes as much as 10 dB at 72.0 Hz (natural frequency of the primary structure).

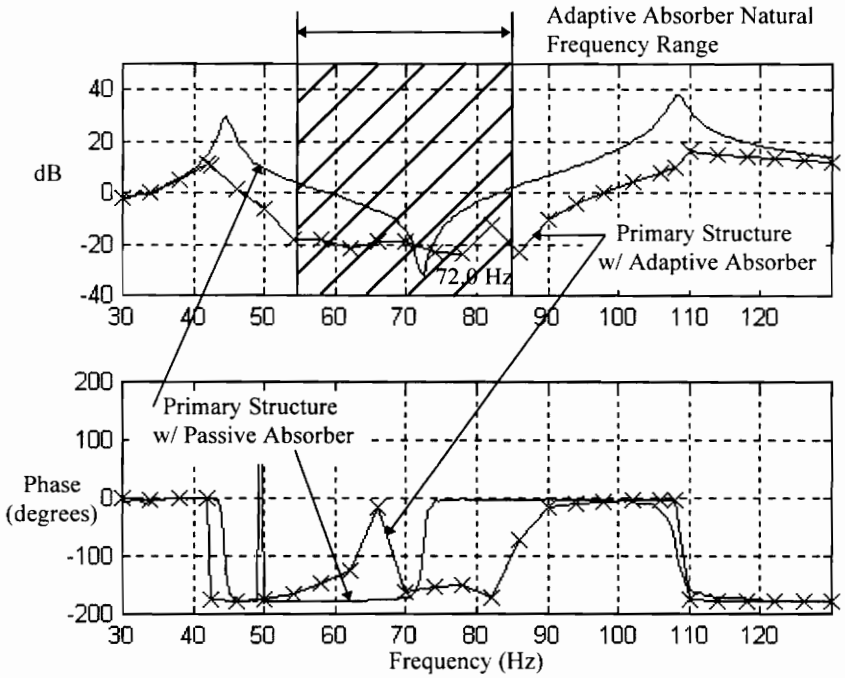

Figure 6.12: FRF of the System: Adaptive vs. Passive (Absorber length = 6.35 cm)

Figure (6.13) shows a comparison of the transfer function plots between the primary structure with no absorber, the primary structure with a passive absorber (tuned to the natural frequency of the primary structure), and the primary structure with an adaptive absorber. As is expected, the system with the adaptive absorber offers significant reduction to the vibration amplitudes, as compared to the other two systems, throughout the 45 Hz to 71 Hz range and the 73 Hz to 108 Hz range. There exists increases in vibration amplitudes throughout the frequency range of 30 Hz to 45 Hz and 110 Hz to 130 Hz for the system with the adaptive absorber as compared to the primary structure with no absorber. However, these increases are still less than the increases that are observed by the system with the passive absorber. The system with the passive absorber offers lower vibration amplitudes for a limited frequency range of 71 Hz to 73 Hz as compared to the system with the adaptive absorber.

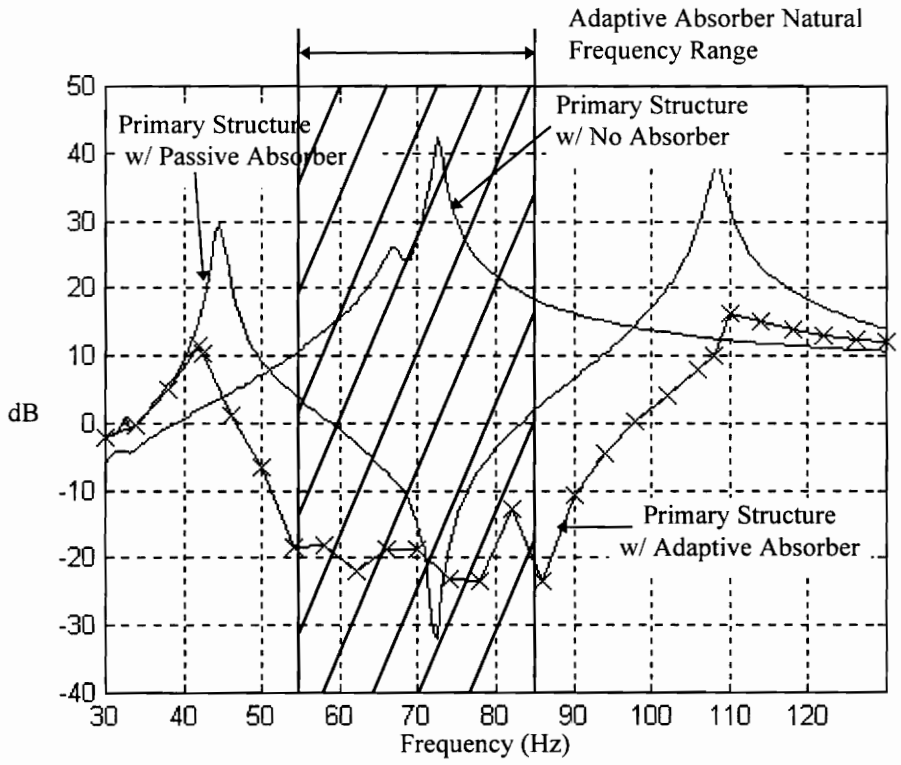

Figure 6.13: FRF of the Primary Structure vs. Adaptive vs. Passive (Absorber length = 6.35 cm)

6.4 Summary

In this chapter we presented the results obtained from our experiments performed in Chapter 5. We presented the results from our preliminary experiments. Next, we presented the results from our adaptive vibration absorber evaluation. Lastly, we presented comparisons for the primary structure with no absorber, primary structure with a passive absorber (tuned to the natural frequency of the primary structure), and the primary structure with an adaptive vibration absorber. In general, the system with the adaptive tuned vibration absorber offered significant vibration amplitude reductions throughout a significant range as compared to the primary structure with no absorber and the primary structure with a passive absorber.

We will conclude our research with Chapter 7. In Chapter 7, we will discuss our conclusions and recommendations for the project.

Chapter 7

7. Conclusions and Recommendations

In this chapter we will present the conclusions for this project and the recommendations for future study or work for this project.

7.1 Conclusions

Our objective for this project was to develop an adaptive absorber located on a primary structure to a forcing frequency applied to the primary structure throughout a frequency range that includes the natural frequency of the primary structure. Also, our objective was to evaluate the final acceleration level obtained by the optimized system. In addition, to keep costs low, the acceleration was evaluated on only one structure. Our objective of this thesis was to create such an absorber system.

In order to accomplish our objective we incorporated a previously designed TVA and made any necessary changes to the TVA to make it adaptive. Next, we obtained the hardware and software necessary to control the system. This involved evaluating different approaches to accomplish the task. Once a solution was found, we proceeded to obtain the necessary equipment.

Once the equipment was obtained, preliminary experiments were done to determine control parameters and instrumentation settings. After the necessary control parameters were known, programming the LabView software to accomplish the control was completed.

The last task of this project was to demonstrate the effectiveness of our adaptive TVA. The primary structure with the adaptive absorber offers significant reduction to the

vibration amplitudes, as compared to the other two systems, throughout both the 45 Hz to 71 Hz range and the 73 Hz to 108 Hz range. There are rare instances where there is an increase in vibration amplitudes for the primary structure with the adaptive absorber as compared to the primary structure with no absorber. This occurs throughout the frequency range of 30 Hz to 45 Hz and 110 Hz to 130 Hz. However, these increases are still less than the increases that are observed by the primary structure with the passive absorber. The primary structure with the passive absorber offers lower vibration amplitudes for a limited frequency range of 71 Hz to 73 Hz as compared to the primary structure with the adaptive absorber.

7.2 Recommendations

Future work for this project could be to incorporate a frequency to voltage converter and eliminate the need for the input voltage source. This would more realistically simulate a real world condition of monitoring a motor frequency and converting it to a voltage value that varies with the frequency.

We also recommend eliminating beam torsion from the design by reorienting the absorber so that it is aligned with the beam and maximizing the effectiveness of the absorber by moving the attachment location of the absorber to the free end of the beam (the location of greatest displacement of the primary structure). This would simplify the theoretical model of the absorber structure and of the combined system as well as allow the absorber to oppose more of the excitation force.

A future test could also evaluate a similar structure with an adaptive absorber that has a larger frequency range. This could be accomplished by replacing the current guiding rods and threaded rod of the adaptive absorber with longer guiding rods and threaded rod. I believe that an absorber with a larger tuning frequency range would result in lower

vibration acceleration levels for the primary structure with the adaptive absorber for frequencies outside the absorber tuning range.

Another comparison, that might yield interesting results, would be to vary the primary structure natural frequency for a given adaptive absorber frequency range. In addition, the experiment would not necessarily have to include the primary structure natural frequency within the absorber tuning frequency range.

References

Desanghere, G., and Vansevenant, E., 1991. "Adaptive tuned Vibration absorber," *Proceedings from the 9th International Modal Analysis Conference Part 2*, Florence, Italy, April 15-18, pp. 1347-1352.

DiDomenico, E., 1994, "Passive Vibration Tuning with Neural Networks," *Proceedings of Smart Structures and Materials.* SPIE. pp. 152-162.

Franchek, M. A., Bernhard, R. J., and Ryan, M., 1993. "Adaptive/Passive Noise and Vibration Control," *AIAA/AHS/ASEE Aerospace Design Conference*. Irvine, California, February 16-19, pp. 1-6.

Hollkamp, J. J., Starchville, T. F., 1994. "A Self-Tuning Piezoelectric Vibration Absorber," Proceedings of the 35th SDM Conference, *AIAA-94-1790*, April 18-22, 1994, Hilton Head, S.C., pp. 521-529.

Intelligent Motion Systems, Inc., 1992. High Performance Microstepper Driver & Indexer *Software Reference Manual*, Taftville, CT.

James, M. L., Smith, G. M., Wolford, J. C., and Whaley, P. C., 1989. Vibration of Mechanical and Structural Systems, Harper & Row, New York.

Lai, J. S., Wang, K. W., 1996. "Parametric Control of Structural Vibrations via Adaptable Stiffness Dynamic Absorbers," *Journal of Vibration and Acoustics*, **118**. January, 1996, pp. 41-47.

Moyka, A. S., 1996. "Adaptive Vibration Absorber," Virginia Polytechnic Institute and State University.

National Instruments Corporation. LabVIEW User's Manual. Austin, Texas, 1994.

Ryan, M. W., Franchek, M. A., and Bernhard, R., 1994. "Adaptive-Passive Vibration Control of Single Frequency Excitations Applied to Noise Control," *Noise-Con.* Ft. Lauderdale, Florida, May, pp. 461-466.

Sun, J. Q., Jolly, M. R., and Norris, M. A., 1995. "Passive, Adaptive and Active Tuned Vibration Absorbers - A Survey," *Transactions of ASME*, **117**. June, 1995, pp. 234-242.

Thomson, W. T., 1993. Theory of Vibrations with Applications, 4th ed., Prentice Hall, New York.

von Flotow, A. H., Beard, A., and Bailey, D., 1994. "Adaptive Tuned Vibration Absorbers: Tuning Laws, Tracking Agility, Sizing, and Physical Implementations," *Noise-Con.* Ft. Lauderdale, Florida, May, pp. 437-454.

Walsh, P. L., and Lamancusa, J. S., 1992. "A variable stiffness vibration absorber for minimization of transient vibrations," *Journal of Sound and Vibration*, **158**(2), pp 195-211. October.

Wang, K. W., Lai, J. S., 1993a. "Control of an Adaptable Dynamic Absorber for Transient Vibration Suppression," *Proceedings of the Second Conference on Recent Advances in Active Control of Sound and Vibration*, pp 506-518.

Vita

Rodney Dale Red Wing was born on April 29, 1968, in Clinton, Missouri. He grew up in Warsaw, Missouri where his parents still reside today. He graduated Warsaw High in 1986. He went to Southwest Missouri State University for pre-engineering studies for two years. He then transferred to the University of Wisconsin - Madison where he obtained his Bachelor of Science degree in mechanical engineering in August of 1994. While at the University of Wisconsin - Madison, he participated in an engineering co-op position with the General Motors Corporation and was also active in the American Indian Science and Engineering Society (AISES) as well as Triangle Fraternity.

In August of 1994, he began his graduate studies at Virginia Polytechnic Institute and State University, where he was financed through a GEM fellowship in addition to a Graduate School and Departmental fellowship. After graduation, he will be employed by General Motors Corporation at the Noise and Vibration Center.